THE JOURNAL OF BIOLOGICAL CHEMISTRY VOL. 287, NO. 9, pp. 6387–6405, February 24, 2012

Insights into Role of Bromodomain, Testis-specific (Brdt) in Acetylated Histone H4-dependent Chromatin Remodeling in Mammalian Spermiogenesis*[S]

Received for publication, August 1, 2011, and in revised form, December 29, 2011 Published, JBC Papers in Press, January 3, 2012, DOI 10.1074/jbc.M111.288167

Surbhi Dhar[1], **Anusha Thota, and Manchanahalli Rangaswamy Satyanarayana Rao**[2]

From the Molecular Biology and Genetics Unit, Jawaharlal Nehru Centre for Advanced Scientific Research, Jakkur, Bangalore 560064, India

Background: Brdt is a double bromodomain containing, testis-specific protein known to recognize acetylated H4.
Results: Smarce1, identified as a novel Brdt interacting partner, shows enhanced interaction upon hyperacetylation of histone H4.
Conclusion: Brdt, a chromatin remodeling factor, associates with Smarce1 in haploid spermatids.
Significance: This study sheds light on the molecular events underlying global chromatin remodeling during mammalian spermiogenesis.

Mammalian spermiogenesis is of considerable biological interest especially due to the unique chromatin remodeling events that take place during spermatid maturation. Here, we have studied the expression of chromatin remodeling factors in different spermatogenic stages and narrowed it down to bromodomain, testis-specific (Brdt) as a key molecule participating in chromatin remodeling during rat spermiogenesis. Our immunocytochemistry experiments reveal that Brdt colocalizes with acetylated H4 in elongating spermatids. Remodeling assays showed an acetylation-dependent but ATP-independent chromatin reorganization property of Brdt in haploid round spermatids. Furthermore, Brdt interacts with Smarce1, a member of the SWI/SNF family. We have studied the genomic organization of *smarce1* and identified that it has two splice variants expressed during spermatogenesis. The N terminus of Brdt is involved in the recognition of Smarce1 as well as in the reorganization of hyperacetylated round spermatid chromatin. Interestingly, the interaction between Smarce1 and Brdt increases dramatically upon histone hyperacetylation both *in vitro* and *in vivo*. Thus, our results indicate this interaction to be a vital step in the chromatin remodeling process during mammalian spermiogenesis.

DNA is present within the eukaryotic nucleus in the form of a highly structured polymer called chromatin, which is composed of a repeating subunit, the nucleosome. Nucleosome has an octet of histones at its core (histones H2A, H2B, H3, and H4 present in two copies each) wrapped around by 1.67 turns of DNA (1, 2). Chromatin is a highly dynamic structure that is constantly remodeled to provide accessibility to several factors facilitating important biological processes. The N-terminal tails of core histones project out of the nucleosome core and are subjected to various post-translational modifications, *vis à vis* acetylation, methylation, phosphorylation, sumoylation, ubiquitination, and others (3, 4). It has thus become a popular belief now that the DNA sequence alone does not decide all possible outcomes of chromatin, and there are factors over and above the defined sequence that lead to various chromatin-templated events. These processes are manifested within the cell in the form of a histone code, which includes post-translational modifications on the nucleosomal histones (5–8). Several chromatin remodeling factors that contain special reader domains within them to recognize such modifications have been identified. Two prominent examples of reader domains are bromodomain and chromodomain. Bromodomain is a small protein domain that can recognize acetylated lysine residues specifically (9), whereas a chromodomain can recognize methylated lysine (10). Over the past few decades, it has come to light that it is not a single modification in isolation, but the combinatorial modification status of the chromatin that serves as the basis of the histone code. This language is transduced in the cell with the help of effector molecules that may be single protein or multiprotein complexes, which carry out the downstream signaling events upon recognition of the histone modifications by reader proteins (11).

In somatic cells, these mechanisms act together to bring about local alterations in the chromatin structure. However, an extreme case of chromatin remodeling occurs during mammalian spermiogenesis where histones are transiently replaced by transition proteins and finally by protamines (12, 13). Several post-translational modifications are known to occur on histones during spermatogenesis, such as acetylation/methylation/phosphorylation/ubiquitination (reviewed in Refs. 14–17) and more recently crotonylation (18, 19). Of these, histone H4 hyperacetylation has long been implicated to be associated with histone removal in rat as it appears just before histone eviction, but the exact mechanism of replacement is still elusive (20, 21). Although spermiogenesis can be divided into 19 morphologically distinguishable steps in rat, it can be broadly divided into

* This work was supported in part by the Department of Biotechnology, New Delhi, India.
[S] This article contains supplemental Table 1 and Fig. 1.
[1] Recipient of fellowship support from the Council of Scientific and Industrial Research.
[2] Recipient of a J. C. Bose fellowship from the Department of Science and Technology. To whom correspondence should be addressed. Tel.: 91-80-2208-2864; Fax: 91-80-2362-2762; E-mail: mrsrao@jncasr.ac.in.

the early, mid, and late elongating spermatid stages. It is after the mid-spermiogenesis step 12 that histones are removed from the chromatin and replaced.

With the objective to understand the chromatin remodeling events that lead to histone removal from elongating spermatids, we studied the expression profile of chromatin remodeling factors in rat. Through our expression data, we picked Brdt[3] as a prospective candidate involved in this chromatin remodeling process. By studying its chromatin remodeling property in haploid spermatids, we observed that it is capable of reorganizing the chromatin in an acetylation-dependent manner, as reported for mammalian cell lines earlier (22). Interestingly, Brdt interacts with Smarce1 (BAF57), which is a member of the SWI/SNF family of ATP-dependent chromatin remodeling complexes through its N terminus. Our data reveal interplay between Smarce1 and Brdt that occurs upon hyperacetylation of haploid spermatid chromatin hinting toward the possible involvement of a remodeling complex in later steps of spermiogenesis.

EXPERIMENTAL PROCEDURES

All fine chemicals were obtained from Sigma and Invitrogen. Other chemicals were purchased from Ranbaxy Chemicals, Qualigens, and Merck. Oligonucleotides were synthesized by Microsynth and Sigma. Anti-acetylated H4 (rabbit polyclonal), anti-H4 (rabbit polyclonal), and anti-acetylated lysine antibodies (rabbit polyclonal) were procured from Upstate Biotechnology, Inc. Anti-phospho-Ser-2/Ser-5 RNA polymerase II antibodies (rabbit polyclonal), anti-TATA-binding protein (mouse monoclonal), anti-Brd2 (goat polyclonal), and anti-GAPDH (rabbit polyclonal) antibodies were obtained from Abcam. Brdt polyclonal antibody was raised in female BALB/c mice using the C-terminal peptide C-NLAREKEQERRRREAMA (position 911–927 amino acids) synthesized at Bio-Concept Laboratories. The anti-Brdt IgG was purified from mouse antiserum using Melon Gel IgG purification kit (Pierce) according to manufacturer's instructions. Anti-Smarce1 (rabbit polyclonal), anti-His (mouse monoclonal), anti-FLAG (mouse monoclonal), anti-α-tubulin (mouse monoclonal), anti-β-actin (mouse monoclonal), and anti-rabbit IgG antibodies were procured from Sigma. Secondary antibodies conjugated with Alexa-488 and Alexa-568 dyes were obtained from Molecular Probes. Protein-A-HRP and secondary antibodies conjugated with HRP were purchased from Bangalore Genei. Recombinant histone H4 (human) was procured from New England Biolabs. Male Wistar rats and female BALB/c mice were obtained from the central animal facility at Indian Institute of Science and animal facility at Jawaharlal Nehru Centre for Advanced Scientific Research, Bangalore, India. All procedures for handling animals were approved by the animal ethics committee of Jawaharlal Nehru Centre for Advanced Scientific Research.

[3] The abbreviations used are: Brdt, bromodomain, testis-specific; HDAC, histone deacetylase; Smarce1, SWI/SNF-related, matrix-associated, actin-dependent regulator of chromatin, subfamily e, member 1; SWI/SNF, switching defective/sucrose nonfermenting; rBrdt, recombinant Brdt; PIS, preimmune serum; Unac, unacetylated; Ni-NTA, nickel-nitrilotriacetic acid; NaBu, sodium butyrate; TSA, trichostatin A.

RNA Isolation and Semi-quantitative and Real Time RT-PCR Analysis—Centrifugal elutriation was performed to isolate tetraploid and haploid cells as reported previously (23). 10-Day-old rat testes were used as a source of gametic diploid cells. Purity of each cell fraction was confirmed by flow cytometry analysis and microscopic visualization upon DAPI staining. Total RNA was isolated from 85 to 90% pure gametic diploid, haploid, and tetraploid cells using TRIzol reagent (Invitrogen) according to the manufacturer's protocol. RNA was given DNase I treatment to remove contaminating genomic DNA, followed by phenol/chloroform extraction. It was quantified spectrophotometrically, and its integrity was checked on a 1% formaldehyde-agarose gel. Random hexamer primers (Sigma) were used to synthesize first strand cDNA using superscript III reverse transcriptase (Invitrogen). A list of 30 chromatin remodeling factors (other than chromatin modifying enzymes) was obtained from the CREMOFAC database, and their mRNA sequences were downloaded from NCBI. Primers listed in supplemental Table 1 were designed using Primer 3 software to amplify a 300–500-bp region. The primers were first tested on total testicular cDNA, and the amplicons were confirmed by DNA sequencing. Semi-quantitative RT-PCR was subsequently performed for each primer set in gametic diploid, tetraploid, and haploid cells. A control reaction without RT was performed to ensure the amplification was not from genomic DNA. Real time RT-PCR analysis for remodeling factors short listed after semi-quantitative RT-PCR analysis was performed three times using iQ SYBER Green dye (Bio-Rad) in an iCycler iQ machine (Bio-Rad). Melt curve analysis was done to ensure specific amplification. Difference in values of threshold cycle (*Ct*) were used to calculate the fold difference in expression of mRNA in gametic diploid, tetraploid, and haploid cells by the $\Delta\Delta Ct$ method ($2^{-\Delta\Delta Ct}$) of analysis. Nascent polypeptide-associated complex α (NACA) was used as an internal normalization control, as its expression level across different spermatogenic cells was found to be unchanged in our microarray experiments.

Western Blotting and Immunocytochemistry—Protein bands resolved by SDS-PAGE were transferred onto nitrocellulose membrane. After transfer, membrane was blocked using 5% skimmed milk powder in phosphate-buffered saline (PBS) for 1 h at room temperature. Subsequently, the membrane was rinsed in wash buffer (0.1% Tween 20 in 1× PBS) three times. This was followed by incubation with the required primary antibody for 2 h at room temperature or overnight at 4 °C. Blots were washed three times in wash buffer and incubated with the appropriate HRP-conjugated secondary antibody (1:3000) or protein-A HRP (1:1000) in a cold room for 2 h. Membranes were washed extensively and developed using the chemiluminescence ECL kit (Thermo Scientific).

For indirect immunofluorescence, adult rat testes were decapsulated and seminiferous tubules digested with collagenase type IV (Sigma) for 20 min. The released cells were washed in PBS and swollen with dithiothreitol according to the method standardized in our laboratory (24). Briefly, total testicular cells were resuspended in decondensation buffer (0.05 mg/ml heparin and 10 mM dithiothreitol in PBS) and incubated on ice for 40 min. Cells obtained after centrifugation were given two washes with 1× PBS. Treated and untreated RAG cells were

trypsinized to be released from the Petri dishes and washed three times in 1× PBS. Treated and untreated round spermatid nuclei were processed for immunofluorescence after performing the remodeling assay with Brdt or M4. The smears were air-dried and fixed in 4% paraformaldehyde for 20 min at room temperature. Autofluorescence was quenched by incubation in 50 mM ammonium chloride for 10 min. Cells/nuclei were permeabilized with 0.1% Triton X-100. They were incubated in the blocking agent (1% BSA in 1× PBS) for 45 min at room temperature followed by incubation in the appropriate primary antibody prepared in 0.1% bovine serum albumin (BSA) for 1 h or overnight in a moist chamber. After washing, secondary antibody (Alexa-488 (green)/Alexa-568 (red)), diluted 1:500 in 0.1% BSA, was added to the smears for 1–2 h. Following washes, nuclei were counterstained with 4′,6′-diamidino-2-phenylindole (DAPI) and mounted in 60% glycerol with antifade. Images were captured in the confocal laser scanning microscope (LSM 510 META, Carl Zeiss). Images and the colocalization data were analyzed by the Zeiss LSM5 image examiner software. Some images were also acquired using the Olympus IX81 inverted microscope.

Cloning, Expression, and Purification of Brdt and Its Deletion Constructs—For expressing *brdt* in a baculovirus expression vector system (Invitrogen), the following steps were followed according to manufacturer's instructions. Full-length rat *brdt* (GenBank™ accession number CH474079) coding sequence (2.8 kb) was cloned in pFastBacHTB vector between EcoRI and NotI sites using the forward primer 5′-ggaattcttatgtctctgccaagtcgac-3′ and reverse primer 5′-atttgcggccgcttaatcaaagttattttcaac-3′. DH10Bac cells were transformed with this construct to allow transposition. Bacmid was isolated from positive clones, transfected in SF-21 cells, and viral particles were generated and amplified. For purification of His-tagged Brdt (rBrdt), SF-21 cells were infected with the viral stocks, and the protein was purified by nickel-nitrilotriacetic acid (Ni-NTA) affinity chromatography.

Brdt deletion constructs M4 (amino acids 1–411), M6 (amino acids 378–947), BD1 (amino acids 20–140), and BD2 (amino acids 260–385) were amplified using the following primers: 5′-gggtttcccatatgatgtctctctgccaagtcgacaaatggctattg-3′ (M4 forward primer) and 5′-cggaattctcagtcatggtctttgtagtcggaagagcagtcccccgagg-3′ (M4 reverse primer); 5′-gggtttcccatatggaacctgttgagagtatgcgtgcat-3′ (M6 forward primer) and 5′-cggaattctcagtcatggtctttgtagtcatcaaagttattttcaaac-3′ (M6 reverse primer); 5′-gggtttcccatatgaatgctaagaaaactgggcggt-3′ (BD1 forward primer) and 5′-cggaattctcagtcatggtctttgtagtcacccacaatctgctcttcctgt-3′ (BD1 reverse primer); and 5′-gggtttcccatatgcacagggttttaaaaacggt-3′ (BD2 forward primer) and 5′-cggaattctcagtcatggtctttgtagtctgcacgcatactctcaacaggt-3′ (BD2 reverse primer). The Brdt deletion constructs were cloned in pET28a(+) vector between NdeI and EcoRI sites containing His_6 sequence at the 5′ end. The reverse primers for each deletion construct were designed to include a 1× FLAG tag sequence in the 3′ end, using p3× FLAG CMV 10 vector (Sigma) as a source for the FLAG sequence. The Brdt deletion constructs were cloned and expressed in *Escherichia coli* BL-21 or Rosetta DE3 cells and purified using Ni-NTA (Qiagen).

In Vitro Remodeling Assays and Interaction Studies—The *in vitro* remodeling activity of rBrdt was assessed using nuclei isolated from RAG cells. Cells in culture were treated with sodium butyrate (NaBu; 4 mM) and trichostatin A (TSA; 125 nM) for 12–16 h, harvested, and washed with PBS. Round spermatids were isolated by centrifugal elutriation and treated with HDAC inhibitors NaBu and TSA in culture as described by us recently (25). Nuclei were purified, and remodeling assay was performed according to the protocol described by Pivot-Pajot *et al.* (22). Briefly, 5×10^6 RAG or round spermatid cells were lysed for 5 min on ice and centrifuged to recover the nuclear pellet. For each remodeling assay, 10^5 untreated or treated nuclei were incubated with 3 μg of full-length Brdt protein (rBrdt) or M4 (N terminus of Brdt) for 1 h at room temperature. Round spermatid nuclei were remodeled in the presence of 1 mM ATP (Fermentas) or 5 units of apyrase (Sigma). The nuclei were mounted on glass slides, fixed with 4% paraformaldehyde, and visualized by DAPI staining.

For interaction studies, remodeling assays were performed on nuclei isolated from 1×10^6 total testicular cells of 45-day-old rats with or without treatment with NaBu and TSA. Flow cytometry analysis depicted the cell population to be 70–75% enriched in haploid cells (data not shown). Nuclear extracts were prepared following the remodeling assay using nuclear lysis buffer (20% glycerol, 20 mM HEPES, 250 mM NaCl, 1.5 mM $MgCl_2$, 0.2 mM EDTA, 1 mM DTT, 0.1% Nonidet P-40, and 0.2 mM PMSF). 15 μl of FLAG M2-agarose beads (Sigma) were incubated with nuclear extracts for 3 h at 4 °C. M2-agarose beads after pulldown were washed four times in nuclear lysis buffer. Five reactions were pooled and loaded on 12% SDS-PAGE after boiling directly in 5× SDS sample buffer. Protein bands were transferred onto nitrocellulose membrane and processed for Western blotting with anti-Smarce1 antibody, anti-acetylated H4 antibody, anti-β-actin antibody, anti-α-tubulin antibody, and anti-GAPDH antibody. Pulldown of M4 protein was confirmed upon reprobing the blot with anti-FLAG antibody.

Preparation of Testicular Nuclear Extracts, Immunoprecipitation, and Mass Spectrometry—Total testicular cells were isolated from 20- and 55–60-day-old rat testes. Round spermatids were collected after centrifugal elutriation. Cells were homogenized in buffer containing 10 mM HEPES (pH 7.4), 1.5 mM $MgCl_2$, 150 mM KCl, 1 mM DTT, and 0.2 mM PMSF, and nuclei were recovered after centrifugation. Sonication-resistant nuclei were prepared from rat testes as described elsewhere (26). Nuclear extracts were prepared using nuclear lysis buffer (20% glycerol, 20 mM HEPES, 250 mM NaCl, 1.5 mM $MgCl_2$, 0.2 mM EDTA, 1 mM DTT, 0.1% Nonidet P-40, and 0.2 mM PMSF). The extracts were quantified and run on 10% SDS-PAGE for immunoblotting with anti-Smarce1 antibody (Sigma). A gel was run in duplicate and stained with Coomassie Blue to confirm equal loading.

For immunoprecipitation, nuclear extracts were prepared from 55- to 60-day-old rat testes. Extracts were quantified, and 1 mg/ml of total nuclear protein was taken for each pulldown reaction. The extracts after preclearing with protein A-agarose beads (Invitrogen) were incubated with 2 μg of rBrdt for 1 h at 4 °C. Immunoprecipitation was performed in parallel with 10

μg of anti-Brdt antibody (mouse) and mock rabbit IgG antibody (Sigma) for 4 h. Protein A-agarose beads after pulldown were washed twice in nuclear lysis buffer and twice in 1× PBST (0.1% Tween 20). Samples were loaded on a 12% SDS-PAGE after boiling directly in 5× SDS sample buffer. The gel was silver-stained using silver staining kit (Invitrogen), and bands that appeared in the pulldown lane were excised. These bands were outsourced to Proteomics International (Australia) for protein identification by MS/MS. Briefly, protein samples were trypsin-digested and peptides extracted according to standard techniques. Peptides were analyzed by electrospray ionization mass spectrometry using the Ultimate 3000 nano-HPLC system (Dionex) coupled to a 4000 Q TRAP mass spectrometer (Applied Biosystems). Tryptic peptides were loaded onto a C18 PepMap100, 3 μm (LC Packings), and separated with a linear gradient of water, acetonitrile, 0.1% formic acid (v/v). Spectra were analyzed to identify proteins of interest using Mascot sequence matching software (Matrix Science) with Ludwig NR database and taxonomy set to rat (*Rattus*). A gel piece having no protein band served as a control.

For Western blotting, the samples after pulldown were run on 10% SDS-PAGE and transferred onto nitrocellulose membrane. Blots were probed with anti-Smarce1 antibody (Sigma).

Chromatin Isolation and ATPase Assay—Round spermatids with or without treatment with HDAC inhibitors in culture were recovered by centrifugation. Cell pellet was washed once with PBS and then briefly with hypotonic buffer containing 10 mM Tris-HCl (pH 7.4), 10 mM KCl, 1.5 mM $MgCl_2$, 0.1 mM PMSF, and β-mercaptoethanol. Subsequently, cell pellet was homogenized in 5 volumes of hypotonic buffer. The nuclear pellet recovered after centrifugation was resuspended in nuclear digestion buffer containing 10% glycerol, 10 mM Tris-HCl (pH 8.0), 3 mM $CaCl_2$, 150 mM NaCl, and 0.2 mM PMSF and digested with micrococcal nuclease (Sigma) at room temperature for 6 min. Reaction was stopped by the addition of EDTA, and samples were incubated on ice for 10 min followed by centrifugation. The chromatin pellet containing oligonucleosomes was resuspended in TE (10 mM Tris and 0.1 mM EDTA) containing 350 mM NaCl and incubated overnight at 4 °C with a 50% slurry of CM-Sephadex on an end to end shaker. Samples were centrifuged, and the supernatant was dialyzed in TE for 8 h with two changes of buffer. The oligonucleosomes isolated from treated (Ac) and untreated (Unac) cells were checked on agarose gel after proteinase K treatment to confirm proper micrococcal nuclease digestion and used subsequently for ATPase assay. The DNA used in the ATPase assay was the 190-bp nucleosome positioning sequence digested and gel-eluted from p208–12 plasmid using EcoRI restriction endonuclease.

Assay for ATPase activity was performed in a 20-μl reaction volume in the following buffer: 20 mM Tris-Cl (pH 7.5), 60 mM KCl, 4% glycerol, 4 mM $MgCl_2$, 1 mM cold ATP (Fermentas), 1 μCi of [γ-^{32}P]ATP (BRIT), and increasing concentrations of recombinant Brdt protein (rBrdt). Where indicated, reaction was supplemented with DNA, untreated oligonucleosomes (Unac), or hyperacetylated oligonucleosomes (Ac). Reactions were performed at 30 °C for 1 h. Free phosphate and ATP were separated by TLC on PEI-cellulose plates (Merck). 1 μl of reaction was spotted on a plate, and TLC was carried out in 1 M formic acid and 0.5 M lithium chloride as solvent. Reactions containing only buffer, only DNA, or only oligonucleosomes were spotted to ensure no background activity was detected. Plates were allowed to air-dry and were visualized by exposure to phosphorimager cassette (Amersham Biosciences) for densitometric analysis.

Genomic Organization of smarce1—The genomic organization of the *smarce1* gene was analyzed across three different organisms as follows: rat, mouse, and human. The *smarce1* exon and intron sequences on rat chromosome 10, mouse chromosome 11, and human chromosome 17 were extracted from three databases, NCBI, Rat Genome Database, and Ensembl, and a schematic diagram representing their organization on respective chromosomes was constructed. Semi-quantitative RT-PCR for *smarce1* splice variants was performed in gametic diploid, tetraploid, and haploid cells using common forward primer 5′-atgtcaaaaagaccatctta-3′ and reverse primer 5′-atcataatcgtctgggtcct-3′.

Cloning, Expression, and Purification of Smarce1 Variants and in Vitro Interaction Studies—Smarce1 sequence (accession number NM_001024993) was retrieved from NCBI, and the ORF was determined using ORF finder software. Smarce1 splice variants were amplified from testis cDNA using the following forward primer 5′-ggatccgaattcgatgtcaaaaagaccatcttatgccc-3′ and reverse primer 5′-atcataatcgtctgggtcct-3′. Amplicons were sequenced and cloned in pET22b(+) vector between EcoRI and XhoI sites. Recombinant proteins containing His_6 tag in the C terminus were purified from *E. coli* and Rosetta DE3 cells by Ni-NTA affinity chromatography.

Immunoprecipitation reactions were carried out using anti-Smarce1 antibody. Rabbit IgG (mock) was used as a control for pulldown. Smarce1 variants (3–4 μg) were incubated individually with 3 μg each of rBrdt, M4, M6, BD1, and BD2 in 1× PBS for 2 h. Simultaneously, protein A-agarose beads (Invitrogen) were incubated with 10 μg of either anti-Smarce1 antibody (Sigma) or rabbit IgG (Sigma). Beads were recovered after centrifugation and added to the proteins for 1 h on end to end rotation at 4 °C. After incubation, beads were given three washes with 0.1% Tween 20 in 1× PBS and boiled directly in 5× SDS sample loading buffer, and the samples were run on 12% SDS-PAGE followed by Western blotting with anti-FLAG antibody (Sigma). Smarce1 pulldown was confirmed by reprobing the blot with anti-Smarce1 antibody. A gel in duplicate was stained with Coomassie Blue to ensure equal loading of Smarce1 variant proteins.

Reverse pulldown experiment was carried out with the FLAG-tagged Brdt mutants M4, BD1, and BD2. 10 μl of FLAG M2-agarose beads (Sigma) were incubated with 3 μg of M4, BD1, or BD2 in PBS for 2 h at 4 °C. 3–4 μg of Smarce1 smaller and larger variant proteins were added separately to each reaction. This was followed by centrifugation to recover the M2-agarose beads and subsequent washes with 0.1% Tween 20 in 1× PBS. The beads were boiled in 5× SDS dye, and samples were separated by 12% SDS-PAGE. Protein bands were transferred onto nitrocellulose membrane and processed for Western blotting with anti-Smarce1 antibody. Because Smarce1 appears next to the IgG heavy chain (~55 kDa) band on the

polyacrylamide gel, the blots were probed with protein A-HRP (Bangalore Genei) instead of secondary antibody conjugated to HRP. Pulldown of Brdt deletion mutants was confirmed upon reprobing the blot with anti-FLAG antibody.

Three-component in Vitro Interaction Studies—In vitro acetylation assays were performed as described elsewhere (27). Briefly, 2 μg of histone H4 (New England Biolabs) was incubated at 30 °C for 4–5 h in a 30-μl final reaction volume consisting of 50 mM Tris-HCl (pH 8.0), 10% (v/v) glycerol, 1 mM dithiothreitol, 1 mM phenylmethylsulfonyl fluoride, 0.1 mM EDTA (pH 8.0), 10 mM sodium butyrate, 8 μM acetyl coenzyme A (Sigma), and recombinant p300 acetyltransferase enzyme (Millipore). 8 μM acetyl coenzyme A was additionally added after 2 h. Pulldown experiment was carried out with the FLAG-tagged Brdt mutant M4. 10 μl of FLAG M2-agarose beads (Sigma) were incubated with 2.5 μg of M4 in 1× PBS for 2 h at 4 °C. This was followed by centrifugation to remove excess M4 protein. Different concentrations of acetylated H4 (0.5 and 1–3 μg) or H4 (0.5 and 1–3 μg) were added separately to each reaction containing 1% Triton X-100 in PBS and incubated for 1 h at 4 °C. Subsequently, 1 μg of Smarce1 was added to each reaction and incubated for 1 h and 30 min. This was followed by centrifugation to recover the M2-agarose beads and subsequent washes with 0.1% Tween 20 in 1× PBS. The beads were boiled in 5× SDS dye, and samples were run on 12% SDS-PAGE. Protein bands were transferred onto nitrocellulose membrane and processed for Western blotting with anti-Smarce1 antibody, anti-acetylated H4 antibody, and anti-H4 antibody. Ponceau S (Sigma) stained blot served as loading control for M4.

RESULTS

During post-meiotic germ cell differentiation, histones from 85 to 90% of the chromatin are removed and replaced by transition proteins (TP1 and TP2) and finally by highly basic proteins called protamines. Considering the scale of chromatin remodeling occurring within these cells is truly global, it is intuitive to suspect the involvement of chromatin remodeling factors that facilitate this process. This study was aimed at identifying chromatin remodeling factors that play a role in mammalian spermiogenesis.

Expression Analysis of Chromatin Remodeling Factors in Spermatogenesis—To begin with the search of such factors, we performed their expression analysis in different spermatogenic cells. The rationale behind this analysis was to search for those remodeling factors that are overexpressed in haploid round spermatids, as these were likely to be involved in chromatin remodeling later in spermiogenesis. The list of chromatin remodeling factors was obtained from CREMOFAC, a database that was developed in our laboratory (28). Tetraploid and haploid germ cell populations were isolated by the method of centrifugal elutriation, and 10-day-old rat testes served as a source of gametic diploid cells (23, 29). RNA was extracted from these cells, and the mRNA expression of 30 chromatin remodeling factors was assessed in them by semi-quantitative RT-PCR analysis (Fig. 1*A*). Thirteen remodeling factors seen expressing in haploid spermatids (Fig. 1*A*) were picked for a more quantitative analysis by real time RT-PCR, to narrow down to the ones that were overexpressed in haploid round spermatids. Five remodeling factors, namely Brdt, Brd2, Baz2a, Smarca2, and Smarce1, were found overexpressing in the haploid spermatids compared with other spermatogenic cells (Fig. 1*B*). Among these, Brdt, a testis-specific chromatin remodeling factor in mammals, belonging to the BET (bromodomains, extra terminal) family consisting of other members like Brd2, Brd3, and Brd4 (30), seemed like a promising candidate. Brdt has been shown earlier to reorganize the chromatin in cultured cells in an acetylation-dependent manner (22). It has also been reported to bind to acetylated histone H4 N-terminal peptides *in vitro* (31) and is postulated to play an important role in spermiogenesis. Hence, we focused our attention on Brdt as the central molecule to address the nature of chromatin remodeling during spermiogenesis in rat.

Brdt Colocalizes with Hyperacetylated Histone H4 in Elongating Spermatids—During spermiogenesis, a key event that takes place in elongating spermatids is the removal and replacement of histones by protamines. It is challenging to understand the mechanisms devised by spermatids to carry out this transition from a nucleohistone- to a nucleoprotamine-based chromatin. In several organisms, a wave of histone acetylation appears in spermiogenesis, just before histone removal. As reported earlier (21), we observed a similar status of histone H4 acetylation in rat spermiogenesis. H4 remained hypoacetylated in the round spermatids; however, there was a dramatic increase in acetylation that began in the early elongating spermatids and continued until mid-elongating stages (supplemental Fig. 1*A*). This signal was not observed in late condensing spermatids because of the removal of histones from these steps. Tetra-acetylated H4 (H4AcK-5, -8, -12, and -16) in somatic cells is considered as a mark of active transcription (32–34). To rule out the possibility of acetylated H4 being correlated with a role in transcription process in elongating spermatids, we performed immunostaining using antibodies against TATA-binding protein and RNA polymerase II phosphorylated at serine positions 2 and 5 to test the status of basal and active transcription, respectively, in these cells. Interestingly, although the basal transcription mark TATA-binding protein could be observed to some degree in very early elongating stages (supplemental Fig. 1*B*), marks for active transcription, RNA polymerase II phosphorylated on serine at position 2 and serine at position 5, were completely absent from the elongating spermatids (supplemental Fig. 1, *C* and *D*, respectively). Thus, the hyperacetylation of H4 observed in early and mid-elongating spermatids is exclusive of transcriptional activity.

We next wanted to investigate the status of Brdt protein expression in spermiogenesis. Toward this objective, antibodies were raised in mouse against Brdt C-terminal peptide-C-NLAREKEQERRRREAMA (position 911–927). Immunocytochemistry experiments done with this antibody indicated the presence of Brdt in all stages of spermiogenesis, from round to elongating spermatids (Fig. 2*A*). In contrast, no signal was observed upon immunostaining with preimmune serum (PIS). The specificity of the antibody was further complemented by an immunoblotting experiment performed on testicular and liver nuclear extracts using anti-Brdt and PIS antibodies (Fig. 2*B*). Although PIS did not pick any protein, anti-Brdt antibody specifically recognized a protein at ~120 kDa in the testes but not

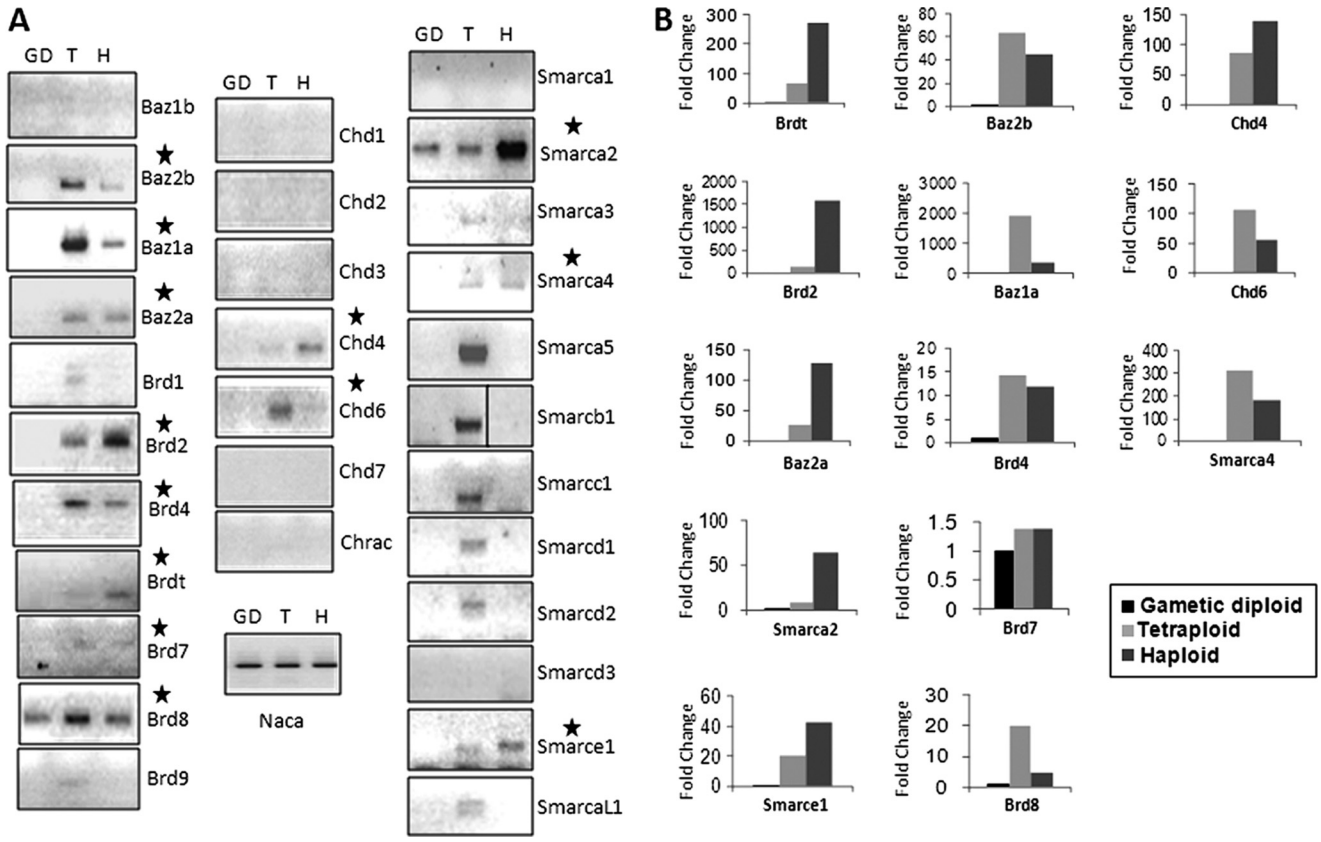

FIGURE 1. **Expression analysis of chromatin remodeling factors in different stages of spermatogenesis.** *A,* semi-quantitative RT-PCR analysis of remodeling factors. Tetraploid and haploid germ cells were isolated by centrifugal elutriation. Testicular cells from a 10-day-old rat represent the gametic diploid cell population. Expression of 30 chromatin remodeling factors was compared among three stages of spermatogenesis, *vis à vis* gametic diploid (*GD*), tetraploid (*T*), and haploid (*H*). The genes that are expressed in haploid spermatids are highlighted with ⋆. *B,* real time RT-PCR analysis of remodeling factors expressing in haploid spermatids. Thirteen remodeling factors were picked for a more quantitative analysis of mRNA expression based on the semi-quantitative RT-PCR data. Fold change in expression for each remodeling factor was compared between gametic diploid, tetraploid, and haploid germ cell stages taking gametic diploid as the reference. NACA1 was used as the normalization control.

liver. Recombinant Brdt protein served as a positive control. Protein expression of Brd2, another BET family member found overexpressing in haploid spermatids (Fig. 1*B*), is restricted to the round spermatids and does not appear in elongating stages (Fig. 2*C*). Thus, it was evident that Brdt is present in stages where H4 becomes hyperacetylated. Through double immunofluorescence analysis, both Brdt and acetylated H4 were observed to colocalize in early and mid-elongating spermatids (Fig. 2, *D* and *E*). Upon quantitative analysis of colocalization, it was observed that the percentage of colocalization increased from 0.5% in the round spermatids to 13.1% in the early elongating spermatids and reached maximum in the mid-elongating spermatids (19.8%), dropping to 0.03% in the late elongating spermatids (Fig. 2, *F* and *G*). This expression study led us to the conclusion that Brdt does recognize acetylated H4 *in vivo* and may play a role in further downstream events taking place in elongating spermatids.

Brdt Can Reorganize Haploid Round Spermatid Chromatin in Acetylation-dependent but ATP-independent Manner—To understand more about the molecular function of Brdt, we cloned the full-length rat *brdt* gene in a baculovirus expression vector system. The expressed recombinant His-tagged protein (rBrdt) was purified using Ni-NTA beads, and its purity was assessed on a Coomassie Blue-stained 12% SDS-PAGE (Fig. 3*A*). To test the activity of the protein, an *in vitro* remodeling assay was performed in cultured RAG cells. RAG cells in culture were treated with HDAC inhibitors NaBu and TSA, and the increase in acetylation was judged by immunostaining with anti-acetylated lysine antibody. The acetylation levels increased in the treated cells when compared with untreated cells (Fig. 3*B*). Furthermore, rBrdt could specifically reorganize acetylated chromatin in the nuclei of treated cells. No changes were seen in the nuclei of untreated cells with or without the addition of rBrdt or treated nuclei in the absence of rBrdt, as judged by DAPI staining (Fig. 3*C*). This property is very reminiscent of the chromatin remodeling reported by Pivot-Pajot *et al.* (22) using a shorter version of murine Brdt (sBrdt).

Even though we could reproduce acetylation-dependent chromatin reorganization by full-length rat Brdt, we were still curious as to the *in vivo* relevance of this property in haploid spermatids. To understand its function *in vivo*, however, was a challenging task because to date there is no system available for the molecular manipulation of haploid spermatids. This is mainly because isolated population of round spermatids is difficult to culture, as they are highly differentiated, nondividing cells (35, 36). Our laboratory has recently established such a system where primary cultures of haploid round spermatids can be maintained at a good viability for 72 h (25). The cells in culture can also be efficiently manipulated by small molecule modulators like the HDAC inhibitors sodium butyrate and tri-

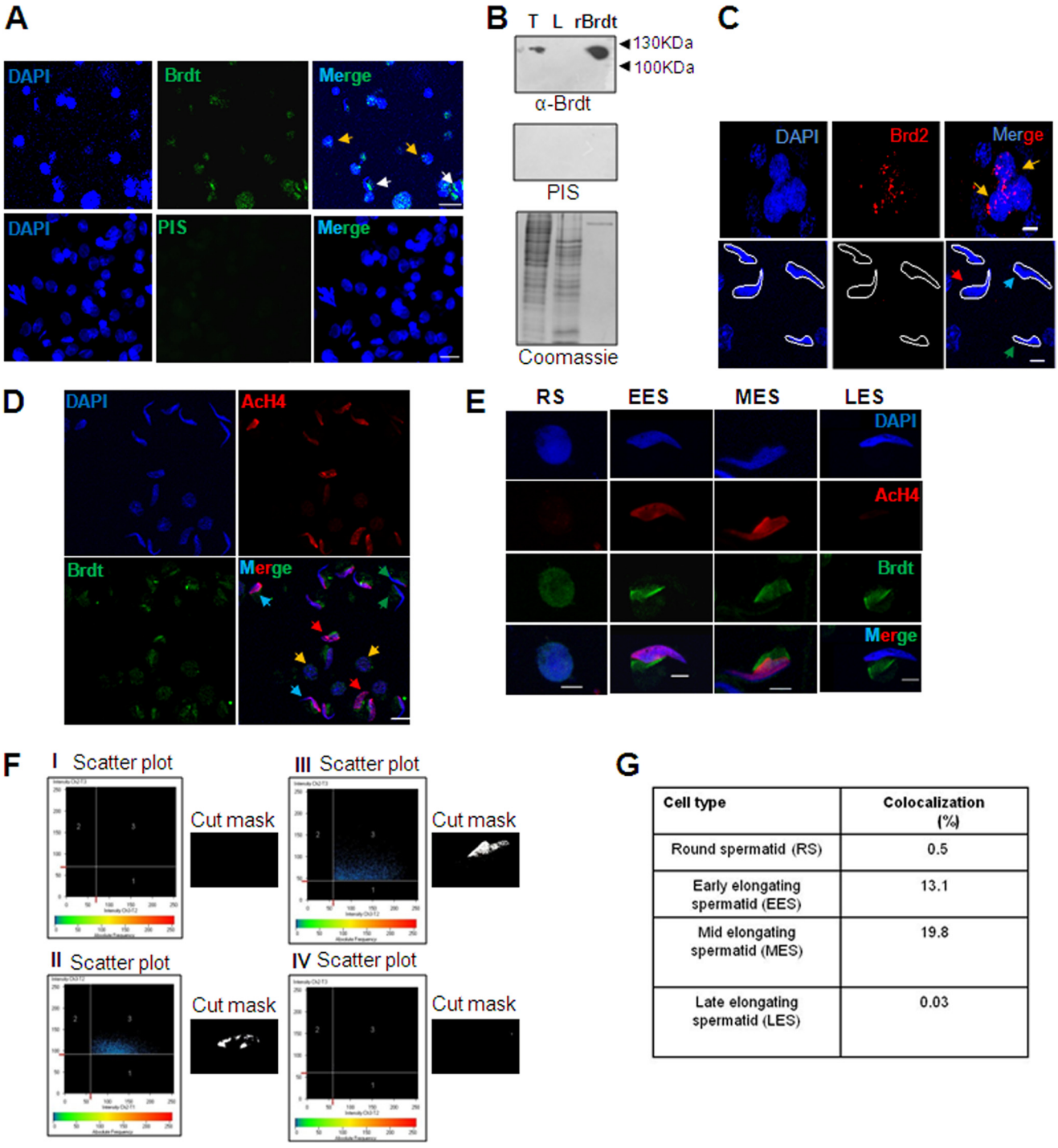

Cell type	Colocalization (%)
Round spermatid (RS)	0.5
Early elongating spermatid (EES)	13.1
Mid elongating spermatid (MES)	19.8
Late elongating spermatid (LES)	0.03

FIGURE 2. **Brdt is present from early to late stages of spermiogenesis and colocalizes with acetylated H4.** *A,* ×40 immunofluorescence image using mouse polyclonal antibody against Brdt showed its presence in different stages of spermiogenesis. *Columns* from *left to right* show fluorescence patterns of DAPI, Brdt, and Merge (DAPI/Brdt). *Yellow arrows* represent round spermatids; *white arrows* represent different steps of elongating spermatids. No signal was detected with PIS. *Scale bars,* 20 μm. *B,* nuclear extracts from testes of a 60-day-old rat (*T*) and liver (*L*) were immunoblotted with the Brdt antibody. A band at ~120 kDa appeared specifically in the testicular extract but not liver. rBrdt was used as a positive control. No such reaction was observed with PIS. A Coomassie Blue-stained gel serves as the loading control. *C,* localization of Brd2 was mapped in spermiogenesis using goat polyclonal antibody (Abcam). *Columns* from *left to right* show fluorescence patterns of DAPI, Brd2, and Merge (DAPI/Brd2). In all panels, *yellow arrows* represent round spermatids; *red arrows*, early elongating spermatids; *blue arrows*, mid-elongating spermatids, and *green arrows*, late elongating spermatids. *Scale bars,* 5 μm. *D,* zoomed ×40 image represents the status of colocalization between acetylated H4 (*red*) and Brdt (*green*) in different spermatogenic cells. In all panels, *yellow arrows* represent round spermatids; *red arrows*, early elongating spermatids; *blue arrows*, mid-elongating spermatids, and *green arrows*, late elongating spermatids. *Scale bar,* 10 μm. *E,* representative ×100 images of spermatogenic cells showing the pattern of colocalization between acetylated H4 (*red*) and Brdt (*green*). *RS* represents round spermatid; *EES* represents early elongating spermatid; *MES* represents mid-elongating spermatid, and *LES* represents late elongating spermatid. *Scale bars,* 5 μm. *F,* analysis of colocalization between acetylated H4 and Brdt. *Panels I–IV* represent the scatter plot analysis and cut mask images for round spermatid, early elongating spermatid, mid-elongating spermatid and late elongating spermatid cells from *E*. The third quadrant in the scatter plot represents the colocalized pixels which are depicted (as *white pixels*) within the cut mask images. *G, table* summarizing the average percentage of colocalization between acetylated H4 and Brdt in different cell types. Data were obtained by performing colocalization analysis on a representative cell from 3 to 5 rounds of immunolocalization experiments. The values remained unchanged even upon switching the fluorophores (*i.e.* acetylated H4 (*green*) and Brdt (*red*)).

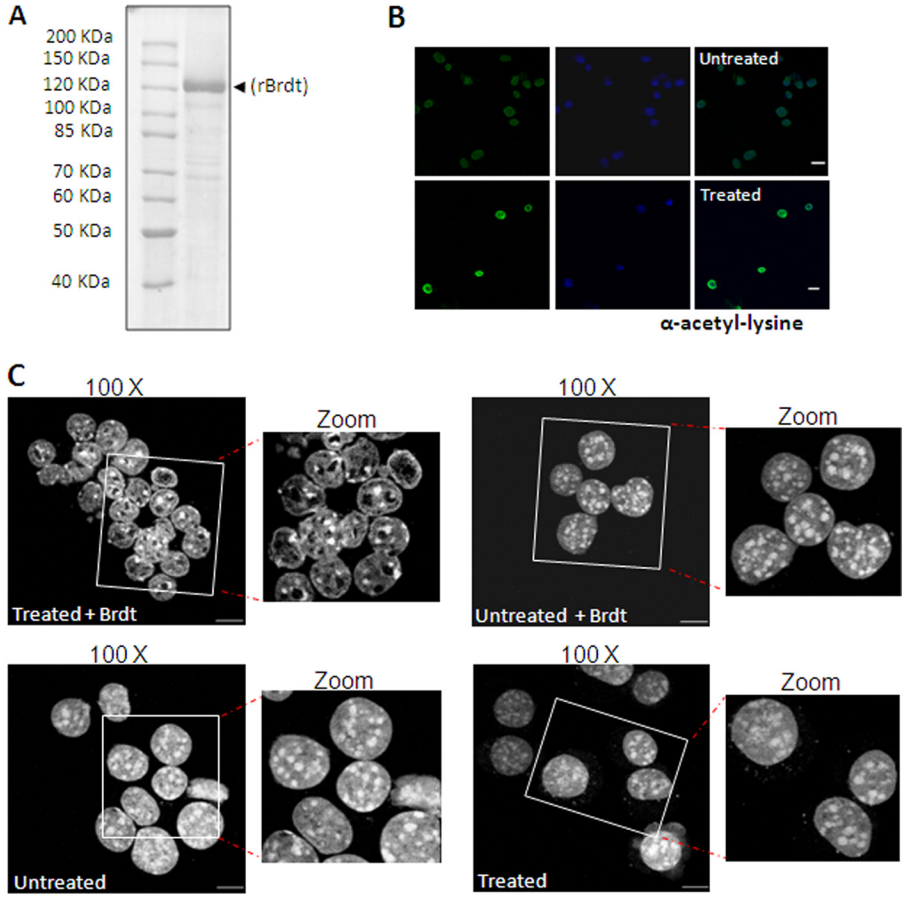

FIGURE 3. ***In vitro* remodeling by Brdt in RAG cells.** *A,* Coomassie-stained image of a 12% SDS-polyacrylamide gel showing recombinant His-tagged Brdt protein, purified from a baculovirus expression vector system. *B,* treated and untreated cells were immunostained with α-acetylated lysine antibody to assess the increase in overall acetylation of RAG cells upon treatment with HDAC inhibitor. *Columns* from *left to right* show fluorescence patterns of acetyl-lysine, DAPI, and Merge (DAPI/Acetyl-lysine) for untreated (*top panel*) and treated (*bottom panel*) RAG cells. *Scale bar,* 10 μm. *C,* comparison of changes in chromatin as observed by DAPI staining upon performing *in vitro* remodeling assay. ×100 and corresponding zoom-in images show nuclei isolated from treated and untreated cells with rBrdt or without rBrdt. *Scale bar,* 10 μm.

chostatin A. Using this system, the function of Brdt could be studied in its natural context, *i.e.* in the haploid spermatids. Remodeling assay in round spermatids gave similar results as obtained with cultured RAG cells. Exogenously added rBrdt could reorganize the chromatin of ~90–95% acetylated round spermatid nuclei, and this property was not observed in the nuclei of untreated cells (Fig. 4*A*). Immunostaining for Brdt confirmed its presence within the nucleus, showing the reorganization in treated nuclei was indeed due to Brdt (Fig. 4*B*). However, even though Brdt was present in untreated nuclei, no chromatin reorganization was observed, reiterating that this chromatin remodeling activity is acetylation-dependent.

Pivot-Pajot *et al.* (22) had reported this property of Brdt to be ATP-independent; however, they had used a C-terminal deletion mutant of murine Brdt. When we carefully studied the amino acid sequence, we found that the rat Brdt protein has a Walker-like motif in its C terminus (GPCGAPGKP). Walker motif A, having the consensus sequence G*XXXX*GKT, is known to bind to ATP. We thought of checking whether the full-length rat Brdt protein possessed any ATPase activity by using [γ-^{32}P]ATP as a substrate. Upon ATP hydrolysis, inorganic phosphate (P_i) should be released, which will move faster than unhydrolyzed ATP when separated by thin layer chromatography. However, Brdt showed no ATP hydrolysis as judged by the ATPase assay (Fig. 4*C*). This activity did not appear upon increasing the concentration of Brdt. The ATPase activity for some proteins can be stimulated in the presence of DNA or chromatin. However, even in the presence of DNA or hypoacetylated (Unac) or hyperacetylated (Ac) round spermatid chromatin, ATPase activity could not be detected for Brdt. Apyrase was used as a positive control in this experiment, showing P_i release upon ATP hydrolysis. On a close analysis of the sequence alignment of Walker motif A with the Brdt C terminus, a proline residue was observed in place of threonine adjacent to the lysine residue in the Walker A-like motif (Fig. 4*D*). Proline is known to cause kinks in the secondary structure, and it is a likely possibility that it may hinder the binding of ATP to lysine, although this hypothesis needs experimental validation. The reorganization of acetylated chromatin by rBrdt was unaltered in the presence or absence of ATP. Treated or untreated round spermatid nuclei showed no changes in their chromatin reorganization upon addition of ATP exogenously or upon depletion of the endogenous ATP pool by apyrase (Fig. 4*A*).

Identification of Smarce1 as an Interacting Partner of Brdt in Rat Testes and Its Expression Analysis—It is now an established fact that chromatin remodeling factors function as multipro-

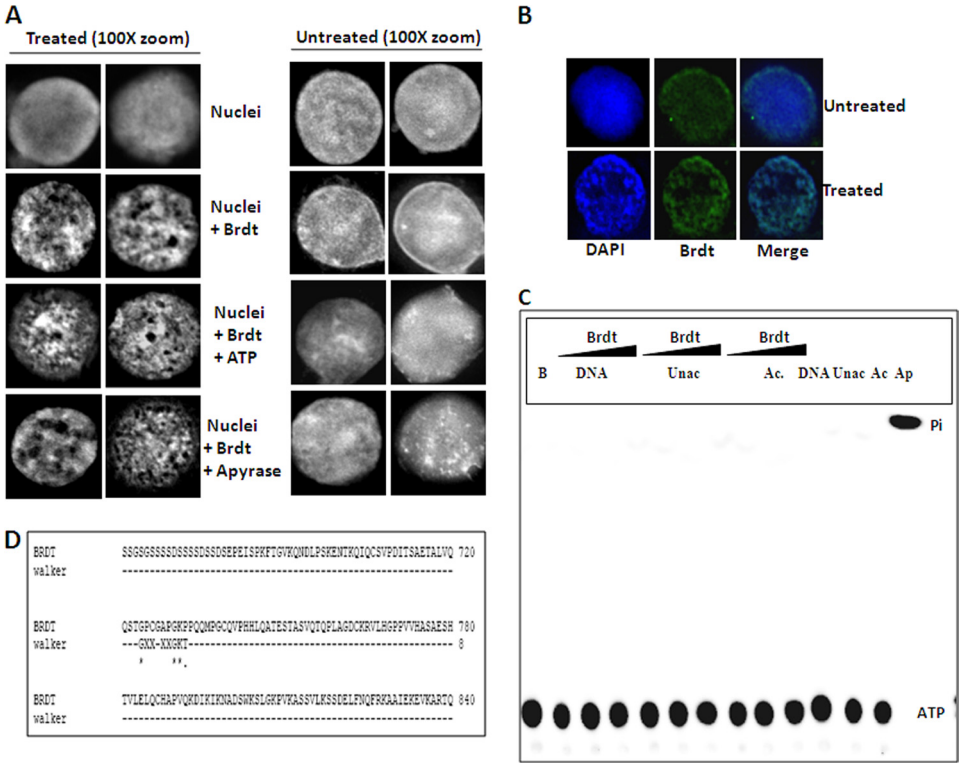

FIGURE 4. ***In vitro* remodeling by Brdt in haploid round spermatids.** *A, in vitro* remodeling assay in haploid round spermatids. Round spermatids in culture were treated with HDAC inhibitors. Nuclei were isolated from untreated and treated cells and incubated with or without recombinant full-length Brdt protein, in the presence of exogenous ATP or upon depletion of endogenous ATP by apyrase. Chromatin reorganization in the nuclei was judged by DAPI staining. Two representative nuclei are shown for each reaction of treated *versus* untreated cells. The experiment was repeated three times. For each experiment, 20 nuclei per reaction were imaged at ×100 and analyzed for changes in chromatin organization. *B,* immunostaining with α-Brdt antibody (mouse) shows the presence of Brdt within the nuclei of both untreated and treated round spermatids. *C,* Brdt was unable to hydrolyze ATP as compared with apyrase (*Ap*), as analyzed by the ATPase assay. This activity did not appear even with increasing concentrations of Brdt in the presence of DNA or Unac or hyperacetylated (*Ac*) oligonucleosomes. Reactions containing only buffer (*B*) or DNA or unacetylated/acetylated oligonucleosomes served as negative controls. *D,* Brdt does not possess any ATPase activity despite the presence of a Walker-like motif in its C terminus, analyzed by the ClustalW software, aligning the consensus Walker motif sequence (G*XXXX*GKT) with the C terminus of Brdt.

tein complexes by interacting with a multitude of accessory interacting protein partners; therefore, we decided to study the interacting partners of Brdt. Immunoprecipitation experiments were performed using anti-Brdt antibody from total testicular nuclear extracts of 55–60-day-old rats enriched in haploid germ cells (Fig. 5*A*). To supplement the concentration of endogenous Brdt, rBrdt was incubated in the nuclear extract before proceeding with the immuno-pulldown. Rabbit IgG served as a negative control (Fig. 5*A*, *bound mock lane*). The bands that appeared exclusively in the pulldown with Brdt antibody (Fig. 5*A*, *bound Brdt lane*) were taken further for analysis by mass spectrometry. The proteins identified by MS/MS analysis have been summarized in Table 1. Many interesting protein partners were identified for Brdt. Of these some were involved in DNA relaxation and repair such as topoisomerase 1 (37–38), splicing factor Pro/Gln-rich (39, 40), and protein-disulfide isomerase A3 (41–43). Heat shock protein 90-α (44, 45) and Hu antigen R (46) are both essential for spermatogenesis as the knock-out mice for both these proteins show defects in post-meiotic spermatid development. Additionally, a few proteins such as heterogeneous nuclear ribonucleoprotein L (47–49) and splicing factor Pro/Gln-rich (50) are known to be involved in splicing. Any nuclear function of endoplasmic reticulum resident protein 44 is not known yet, but like protein-disulfide isomerase A3 (Erp57), it may have a moonlighting role in the nucleus. Only two proteins are known to have direct effects on chromatin organization as part of chromatin remodeling complexes. These are Smarce1 (51–56) and β-actin (57–60). We got particularly interested in Smarce1, as it was one of the five chromatin remodeling factors found overexpressing in haploid germ cells, as shown by real time RT-PCR analysis (Fig. 1*B*). To confirm the interaction of Smarce1 with Brdt, Western blotting was done after anti-Brdt pulldown from 60-day-old rat testicular nuclear extracts using anti-Smarce1 antibody. A band at ~55 kDa corresponding to Smarce1 was indeed observed in the pulldown lane as compared with the control lane (Fig. 5*B*).

Primers were designed against the coding sequence of rat *smarce1* gene to clone it from testis cDNA. Interestingly, two bands appeared in the agarose gel at 1.2 and 1.1 kb upon PCR amplification. Semi-quantitative RT-PCR analysis in diploid, tetraploid, and haploid cells revealed that the lower band (444 bp) started to appear from the tetraploid stage onward and continued into haploid cells. Expression of the upper band at 549 bp (444 + 105 bp), however, remained almost constant with a slight decrease in the haploid spermatids (Fig. 6*A*). Correspondingly, a Western blot analysis across different spermatogenic stages was done with anti-Smarce1 antibody on nuclear extracts from 20- and 55-day-old rat testis, round spermatids, and sonication-resistant spermatids (Fig. 6*B*). The germ cells in the testis of 20-day-old rats represent the diploid spermatogo-

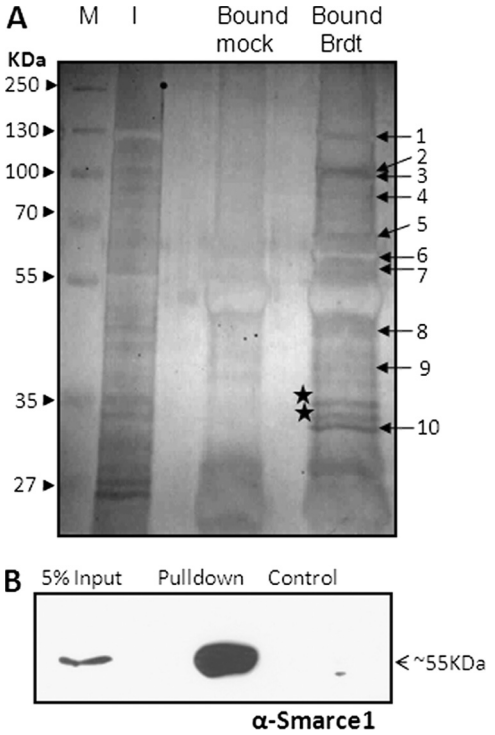

FIGURE 5. **Smarce1, an interacting partner of Brdt in rat testes.** *A,* immunopulldown of rBrdt and its associated interacting proteins. rBrdt was incubated with total testicular nuclear extracts from 55- to 60-day-old rat and immunoprecipitated using mouse polyclonal α-Brdt antibody (*lane Bound Brdt*). Rabbit IgG was used for mock pulldown (*lane- Bound Mock*). *Lane I* represents 20% of the total testicular nuclear extract used for pulldown with rBrdt. Samples were run on 12% SDS-PAGE, silver-stained, and analyzed by mass spectrometry. *Arrows* indicate the proteins identified by mass spectrometry (summarized in Table 1). Bands that are highlighted (⋆) could not be identified. *Lane M*, marker lane. *B,* Brdt and Smarce1 interaction was confirmed by Western blot analysis using α-Smarce1 antibody after rBrdt immuno-pulldown from testicular nuclear extracts. Pulldown with rabbit IgG served as control.

nia and early pachytene spermatocytes; those from 55-day-old rats contain predominantly post-meiotic haploid spermatids. Purified populations of round spermatids were obtained after centrifugal elutriation, and sonication-resistant spermatids represent the elongating and condensing spermatid stages. Two protein bands appeared at ~55 kDa, correlating well with the two DNA bands seen in the semi-quantitative RT-PCR analysis. Although both bands were present relatively equally in 20-day-old rat testis (Fig. 6*B, 20d lane*), 55-day-old rat testis (*55d lane*), and round spermatid (*RS lane*) nuclear extracts, the lower band was more prominent in the sonication-resistant spermatids (*SRS lane*). Another unidentified band was observed below 35 kDa, the expression of which progressively decreased across spermatogenesis. To understand if Brdt and Smarce1 have a functional overlap in elongating stages of spermiogenesis, their protein expression was mapped in spermiogenesis by immunofluorescence. Although Smarce1 was present in all stages of spermiogenesis from round spermatids to late elongating spermatids, it was found to colocalize with Brdt primarily in mid-elongating spermatids (Fig. 6, *C* and *D*). Quantification of Smarce1 and Brdt colocalization revealed a dramatic increase only in the mid-elongating spermatids (Fig. 6, *E* and *F*).

Genomic Organization of Smarce1 and Identification of Its Splice Variants in Spermatogenic Cells—Because the two DNA bands in the agarose gel at 1.1 and 1.2 kb corresponded well with the two protein bands observed in the Western blot, for Smarce1 we thought these could be variants of the *smarce1* gene. To test this hypothesis, we analyzed the genomic organization of *smarce1* on the rat chromosome 10. However, the sequence of this chromosome is not fully annotated in NCBI, Ensembl, or Rat Genome Database. When compared with human and mouse *smarce1* gene sequences, the third exon in rat *smarce1* had three bases (ACA) and the sixth exon had 31 bases (from GTC to CTG) missing. These sequences are present in the *smarce1* rat coding sequence as given in the NCBI database and corroborated with our DNA sequencing analysis. The intron/exon boundaries from the sequence of intron 5 were absent, and the sequence from tenth intron onward was not available. The 5′ upstream sequence of the first exon was also unavailable. Hence, the information available for introns and exons of *smarce1* gene on human chromosome 17 and mouse chromosome 11 was used to construct the schematic diagram for *smarce1* genomic organization on rat chromosome 10. The diagram representing the *smarce1* gene on the human, mouse, and rat chromosomes, with its introns (*white boxes*) and exons (*black boxes*), is given in Fig. 7*A*. The sequencing results of the two bands are shown in Fig. 7*B*. An additional 105-bp insertion in the *smarce1* larger variant cDNA sequence in Fig. 7*B* is highlighted in *red*. This sequence matches exactly with the sequence of the fourth exon of *smarce1*. We therefore conclude that the two sequences in question are alternately spliced variants of *smarce1* with the smaller variant being generated by splicing of the fourth exon. The region that is spliced out in the smaller variant is marked by a *gray box* in Fig. 7*A*.

Brdt Interacts with Smarce1 via Its N terminus in Vitro—To map the domain(s) of Brdt involved in its interaction with Smarce1, we constructed deletion mutants of Brdt. Brdt mutants M4 (representing the N terminus), M6 (representing the C terminus), BD1 (representing the first bromodomain), and BD2 (representing the second bromodomain) were expressed with a His tag in the N terminus and a FLAG tag in the C terminus. Because it has not yet been established which of the two variants of Smarce1 interacts with Brdt *in vivo*, interaction experiments were performed *in vitro* with both the variants. Smarce1 variants were cloned, expressed, and purified from BL-21 cells, and immunoprecipitation was done in its *in vitro* reactions with rBrdt, M4, M6, BD1, and BD2, using Smarce1 antibody (immunoprecipitation). To confirm the pulldown of Smarce1, blots were probed with anti-Smarce1 antibody. Furthermore, Western blotting with anti-FLAG antibody was performed to detect the status of pulldown of Brdt mutants, whereas anti-His antibody was used to detect the full-length rBrdt pulldown. Rabbit IgG was used as a negative control for pulldown (IgG). It was observed that the full-length Brdt could interact with both the Smarce1 variants *in vitro* (Fig. 8*A*). Our interaction experiments also revealed that the N terminus of Brdt, which spans amino acids 1–411 encompassing both the bromodomains (BD1 and BD2), interacts with Smarce1, whereas no interaction

TABLE 1
Proteins associated with rBrdt

No.	Protein name	Swiss-Prot (UniProtK B)	Total peptides	Peptides[a]	Mass (UniprotKB)	Contextual functions (with corresponding references)
1	Brdt	Brdt Rat (D4A7T3)	42	K.SVLPDSQQQHR.V R.EFGSGFTPESSSNKVOGR.S K.LEEEDNAKPMNYDEKR.Q R.NSNPDEIEIDFETLK.A K.DACEFAADVR.L	106.7 kDa	Acetylation-dependent chromatin remodeling (16.25), essential for proper spermatogenesis (58)
2	DNA Topoisomerase 1	Top 1 Rat (Q9WUL0)	14	K.ENGFSSPPR.I R.TYNASITLQQQLK.E K.AEEVATFFAK.M K.ELTAPDENVPAK.I K.YIMLNPSSR.I	90.7 kDa	DNA relaxation (34). Nucleosome disassembly (35)
3	Splicing factor P/Q-rich (PTB protein associated)	Sfpq Rat (Q4KM71)	13	R.FGQGGAGPVGGOGPR.G R.SPPPGMGLNQNR.G K.GIVEFASKPAAR.K K.YGEPGEVFINKGK.G K.AELDDTPMR.G	75.4 kDa	Stimulates DNA topoisomerase 1 (36), DNA double strand break rejoining (37), Splicing (47)
4	Heat shock protein HSP 90-α	Hsp90-α rat (P82995)	15	R.GVVDSEDLPLNISR.E R.ELISNSSDALDK.I R.TLTIVDTGIGMTK.A K.HLEINPDHSIIETLR.Q R.NPDDITNEEYGEFYK.S	84.8 kDa	Interacts with HSP70 in mouse testes (41) Molecular chaperone required for post-meiotic progression in spermatogenesis (42)
5	Heterogeneous nuclear ribonucleoprotein L	Hnmpl Rat (F1LPP9)	41	R.SSSGLLEWDSK.S K.SKPGAAMVEMADGYAVDR.A R.AITHLNNNFMFGQK.M K.NGVQAMVEFDSVQSAQR.A R.KNGVQAMVEFDSVQSAQR.A	67.9 kDa	Splicing (44–46)
6	Protein-disulfide isomerase A3	Pdia3 Rat (P11598)	15	R.LAPEYEAAATR.L K.IFRDGEEAGAYDGPR.T K.LNFAVASR.K R.DGEEAGAYDGPR.T R.ELNDFISYLQR.E	56.6 kDa	DNA binding (38, 40), DNA-damage response (39)
7	SWI/SNF-related, matrix-associated, actin-dependent regulator of chromatin, subfamily e, member 1	Smarce 1 Rat (Q56A18)	1	K.FLESTDSFNNELKRLCGL.K	42.8 kDa	Subunit of SWI/SNF ATP-dependent chromatin remodeling complexes (48–53)
8	Endoplasmic reticulum resident protein 44 precursor	Erp44 Rat (F1M396)	3	K.LAPSEYR.Y R.NIIGYFEOK.D R.YSGDNLIYKPPGR.S	46.7 kDa	
9	β-Actin	ActB Rat (P60711)	13	K.SYELPDGOVITIGNER.F K.QEYDESGPSIVHR.K K.DSYVGDEAQSKR.G K.QEYDESGPSIVHR.K K.SYELPDGQVITIGNER.F	41.7 kDa	Subunit of chromatin remodeling complexes in the nucleus (54–57)
10	ELAV (embryonic lethal, abnormal vision, *Drosophila*)-like 1 (Hu antigen R)	Elavl1 Rat (B5DF91)	1	R.VLVDQTTGLSR.G	36.1 kDa	Essential at meiotic and post-meiotic stages of spermatogenesis; regulates levels of HSP70–2 (43)

[a] First five unique peptides with the highest score are shown.

was detected with the C terminus of Brdt (amino acids 378–947; including the extra-terminal domain). Interestingly, both the bromodomains of Brdt, BD1 and BD2, also interacted with Smarce1 variants.

To confirm the Brdt domains involved in interaction with Smarce1, we carried out reverse pulldown experiments. The interaction results held true in the reverse pulldown as well, in which FLAG-tagged mutants of Brdt, *i.e.* M4, BD1, and BD2, were immunoprecipitated using FLAG-M2-agarose beads (Fig. 8*B*). To analyze pulldown of Smarce1, the blots were probed with anti-Smarce1 antibody. The interaction of Smarce1 variants with M4, BD1, and BD2 could be reproduced in this experiment, validating the results of pulldown with Smarce1 antibody (Fig. 8*A*). To ensure equal concentration of Smarce1 was added to each reaction, a 12% SDS-PAGE was performed in parallel as loading control (see Fig. 8, *A* and *B*).

Interaction of Smarce1 with M4 (Brdt N Terminus) Is Enhanced in Presence of Acetylated H4—To test the possibility of interaction between Smarce1 and Brdt being modulated by acetylated H4, we resorted to a three-component interaction system. M4 was incubated with increasing concentrations of acetylated or unacetylated H4. This was followed by addition of a subequimolar concentration of recombinant Smarce1 protein. Pulldown was performed for FLAG-tagged M4 protein using M2-agarose beads. When the blots were probed after pulldown with anti-acetylated H4 antibody, an expected gradual increase was observed in the band intensity that was not seen for unacetylated H4 (Fig. 9). Interestingly, a similar increase was observed in Smarce1 signal in the presence of increasing concentrations of acetylated H4 (Fig. 9, *lanes 1–4*). The Smarce1 band intensity remained unchanged upon increasing concentrations of unacetylated H4 (Fig. 9, *lanes 6–9*). The intensity of the

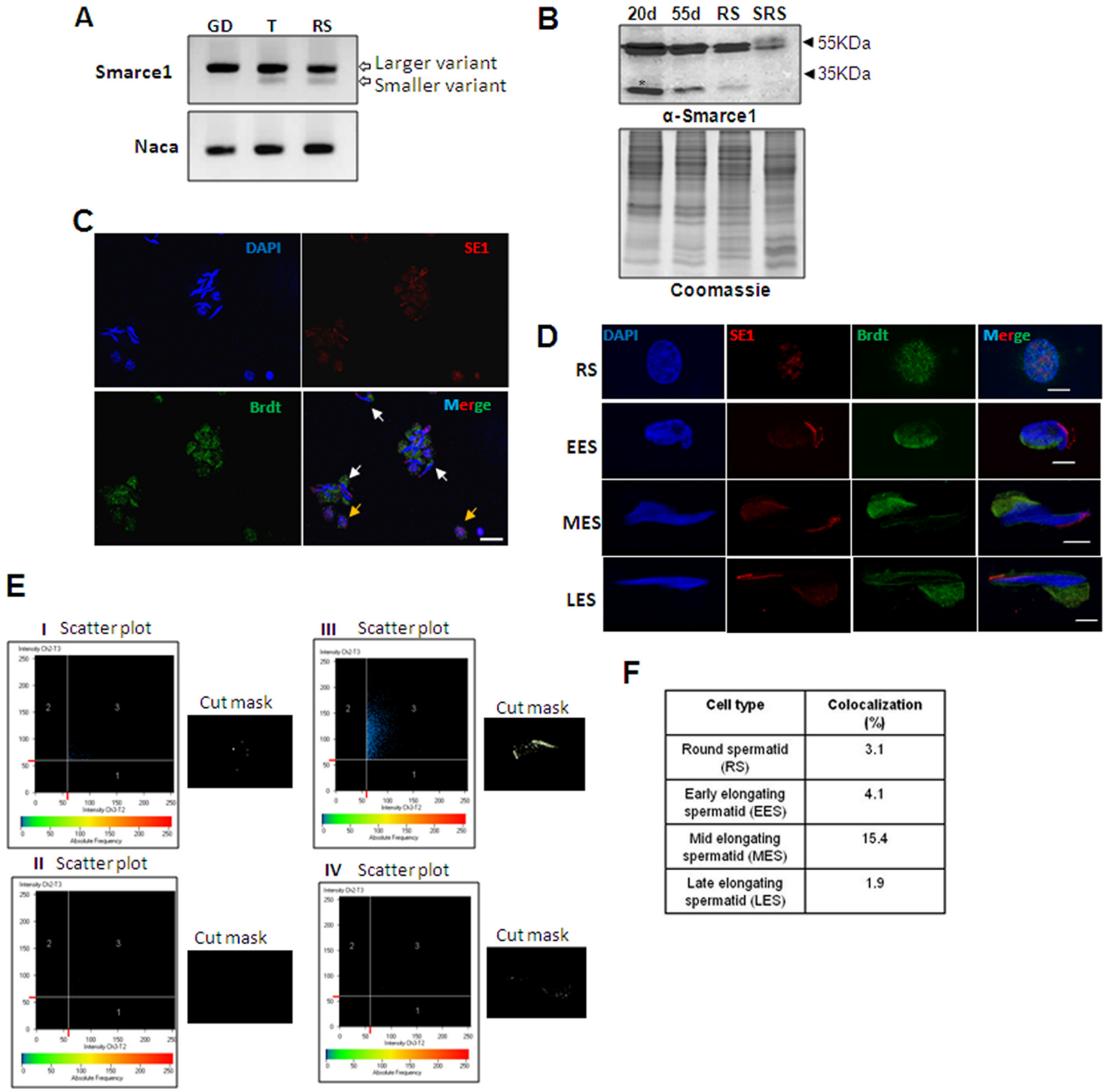

Cell type	Colocalization (%)
Round spermatid (RS)	3.1
Early elongating spermatid (EES)	4.1
Mid elongating spermatid (MES)	15.4
Late elongating spermatid (LES)	1.9

FIGURE 6. **Expression analysis of Smarce1.** *A*, semi-quantitative RT-PCR was performed using primers designed to specifically check the expression of *smarce1* splice variants in different stages of spermatogenesis, *i.e.* gametic diploid (*GD*), tetraploid (*T*), and round spermatids (*RS*). Nascent polypeptide-associated complex α was used as a housekeeping control. *B,* Western blotting revealed the status of protein expression across spermatogenesis in 20-day-old rat testes (*20d*), 55-day-old rat testes (*55d*), round spermatids (*RS*), and sonication-resistant spermatids (*SRS*) nuclear extracts. Two variants of Smarce1 were observed at ~55 kDa, and another band was seen below 35 kDa. *Lower panel* represents the nuclear extracts of 20-day-old rat testis (*20d*), 55-day-old rat testes (*55d*), round spermatids (*RS*), and sonication-resistant spermatids (*SRS*) on a Coomassie Blue-stained gel as loading control. *C,* a ×40 image represents the status of colocalization between Smarce1 (*red*) and Brdt (*green*) in different spermatogenic cells. *Yellow arrows* represent round spermatids; *white arrows* represent different steps of elongating spermatids. *Scale bar,* 20 μm. *D,* representative ×100 images of spermatogenic cells showing the pattern of colocalization between Smarce1 (*red*) and Brdt (*green*). *RS* represents round spermatid; *EES* represents early elongating spermatid; *MES* represents mid-elongating spermatid, and *LES* represents late elongating spermatid. *Scale bars,* 5 μm. *E,* analysis of colocalization between Smarce1 and Brdt. *Panels I–IV* represent the scatter plot analysis and cut mask images for round spermatid, early elongating spermatid, mid-elongating spermatid, and late elongating spermatid cells from *D*. The third quadrant in the scatter plot represents the colocalized pixels which are depicted (as *white pixels*) within the cut mask images. *F, table* summarizing the average percentage of colocalization between Smarce1 and Brdt in different cell types. Data were obtained by performing colocalization analysis on a representative cell from 3 to 5 rounds of immunolocalization experiments. The values remained unchanged even upon switching the fluorophores (*i.e.* Smarce1 (*green*) and Brdt (*red*)).

Smarce1 bands (Fig. 9, *lanes 6–9*) was equal to that observed in *lane 5*, which represents the interaction between Smarce1 and Brdt in the absence of H4 proteins. This indicates that unacetylated H4 does not hinder this interaction; moreover, acetylated H4 enhances it.

Significance of Smarce1 and Brdt Interaction in Vivo—Having established a physical association between Brdt and Smarce1 in an *in vitro* interaction system, we were curious to know the significance of this interaction in the *in vivo* context. To understand if Smarce1 associates with Brdt in its chromatin

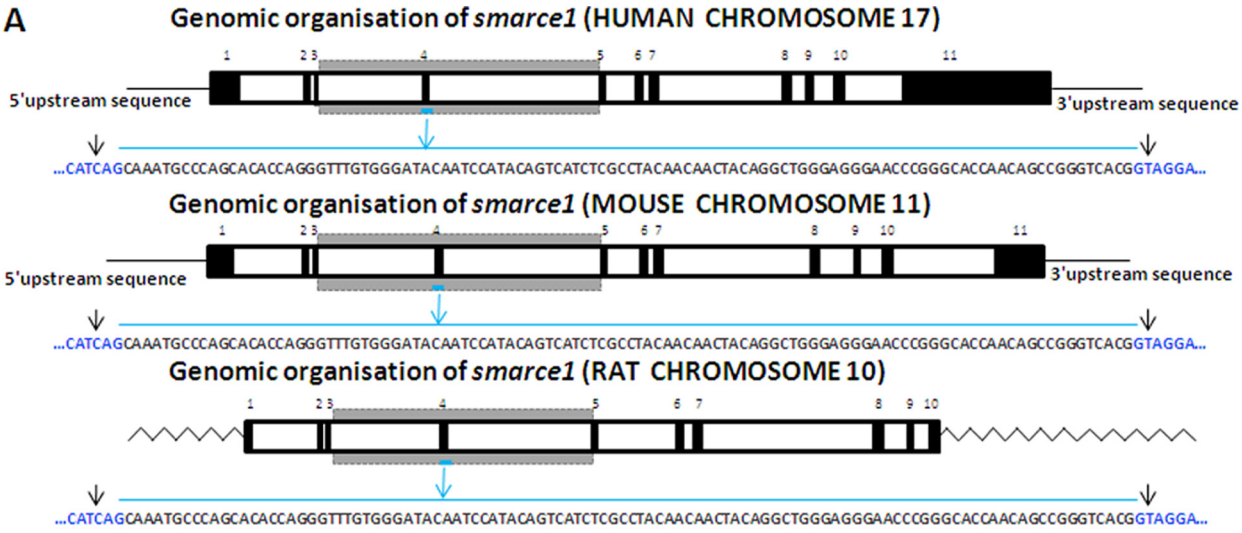

B

smarce 1 smaller variant

ATGTCAAAAAGACCATCTTATGCCCCACCTCCCACCCCAGCTCCTGCAACAGCGTCCTCCGGCATTACAATCCCAAAGCCTCCAAAGCCACCAGATAAGCCGCTCATGCCCTACATGAGGTACAGCAGAAAGGTCTGGGACCAAGTA
AAGGCTTCCAACCCTGACCTAAAGTTGTGGGAGATTGGCAAGATTATTGGTGGCATGTGGCGAGATCTCACTGATGAAGAGAAACAAGAATATTTAAACGAGTACGAAGCAGAAAAGATAGAGACAATGAATCTATGAAGGCCTA
TCACAATTCCCCTGCATACCTTGCATATATTAATGCAAAAAGTCGTGCGGAAGCTGCATTAGAGGAAGAAAGTCGACAGAGACAGTCGCGCATGGAGAAAGGAGAGCCTTACATGAGCATTCAGCCTGCGGAGGACCCAGACGAT
TATGATGACGGCTTTTCAATGAAGCATACAGCCACTGCCCGTTTCCAGAGAAACCACCGCCTCATCAGTGAGATCCTCAGTGAGAGTGTGGTACCTGATGTGCGGTCGGTTGTCACAACAGCTAGAATGCAAGTCCTCAAGCGACAG
GTCCAGTCTTTAATGGTTCATCAGCGGAAACTAGAAGCCGAGCTTCTTCAGATAGAGGAACGACACCAGGAAAAGAAGAGGAAATTCCTGGAAAGCACAGACTCCTTTAACAATGAGCTTAAAAGGCTGTGTGGTCTGAAGGTGG
AAGTGGACATGGAGAAGATTGCAGCAGAGATCGCACAGGCGGAGGAGCAGGCCCGCAAAAGGCAGGAGGAGAGGGAGAAGGAGGCAGCCGAGCAAGCTGAGCGCAGCCAGGGCAGCATCGCCCCCGAGGAAGAGCAAGTG
GCGAACAAAGCCGAGGAGAAGAAGGATGAGGAGAACATCCCGATGGAGACAGAGGAGACACACCTTGAAGACACTGCGGAGAACCAGCAGAATGGTGAAGAAGGCACATCTACTCCTGAGGACAAGGAGAGTGGGCAGGAG
GGGGTTGACAGCATGGAGGTGGAAGGGACCAGTGACAGTAACACCGGCTCAGAGAGCAACAGCGCAACGGTGGAGGAGCCGCCCACGGACCCTGTGCCAGAAGACGAGAAGAAGGAATAA

smarce 1 larger variant (with additional 105 bp sequence)

ATGTCAAAAAGACCATCTTATGCCCCACCTCCCACCCCAGCTCCTGCAACACAAATGCCCAGCACACCAGGGTTTGTGGGATACAATCCATACAGTCATCTCGCCTACAACAACTACAGGCTGGGAGGGAACCCGGGCACCAACAGC
CGGGTCACGGCGTCCTCCGGCATTACAATCCCAAAGCCTCCAAAGCCACCAGATAAGCCGCTCATGCCCTACATGAGGTACAGCAGAAAGGTCTGGGACCAAGTAAAGGCTTCCAACCCTGACCTAAAGTTGTGGGAGATTGGCAA
GATTATTGGTGGCATGTGGCGAGATCTCACTGATGAAGAGAAACAAGAATATTTAAACGAGTACGAAGCAGAAAAGATAGAGTACAATGAATCTATGAAGGCCTATCACAATTCCCCTGCATACCTTGCATATATTAATGCAAAAA
GTCGTGCGGAAGCTGCATTAGAGGAAGAAAGTCGACAGAGACAGTCGCGCATGGAGAAAGGAGAGCCTTACATGAGCATTCAGCCTGCGGAGGACCCAGACGATTATGATGACGGCTTTTCAATGAAGCATACAGCCACTGCCC
GTTTCCAGAGAAACCACCGCCTCATCAGTGAGATCCTCAGTGAGAGTGTGGTACCTGATGTGCGGTCGGTTGTCACAACAGCTAGAATGCAAGTCCTCAAGCGACAGGTCCAGTCTTTAATGGTTCATCAGCGGAAACTAGAAGCC
GAGCTTCTTCAGATAGAGGAACGACACCAGGAAAAGAAGAGGAAATTCCTGGAAAGCACAGACTCCTTTAACAATGAGCTTAAAAGGCTGTGTGGTCTGAAGGTGGAAGTGGACATGGAGAAGATTGCAGCAGAGATCGCACAG
GCGGAGGAGCAGGCCCGCAAAAGGCAGGAGGAGAGGGAGAAGGAGGCAGCCGAGCAAGCTGAGCGCAGCCAGGGCAGCATCGCCCCCGAGGAAGAGCAAGTGGCGAACAAAGCCGAGGAGAAGAAGGATGAGGAGAACAT
CCCGATGGAGACAGAGGAGACACACCTTGAAGACACTGCGGAGAACCAGCAGAATGGTGAAGAAGGCACATCTACTCCTGAGGACAAGGAGAGTGGGCAGGAGGGGGTTGACAGCATGGAGGTGGAAGGGACCAGTGACAGT
AACACCGGCTCAGAGAGCAACAGCGCAACGGTGGAGGAGCCGCCCACGGACCCTGTGCCAGAAGACGAGAAGAAGGAATAA

FIGURE 7. **Splice variants of Smarce1.** *A,* genomic organization of *smarce1* gene on human chromosome 17, mouse chromosome 11, and rat chromosome 10 is shown. The information on the rat chromosome 10 was not fully available, hence the human and mouse *smarce1* genomic organization was used as reference. The *black boxes* represent the exons, and the *white boxes* represent the introns. The region including the fourth exon, which is spliced to give rise to the smaller variant, is highlighted in the *gray box*. The 105-bp sequence of the fourth exon and start of intron boundaries (*blue*) is depicted. *B,* sequence of the *smarce1* splice variants. The bands at 1.13 kb (smaller variant) and 1.236 kb (larger variant) shown in Fig. 6*C* were sequenced. The 105-bp additional sequence in the larger variant (shown here in *red*) exactly matches the sequence of the fourth exon.

remodeling function, we resorted to the chromatin remodeling assay established in the round spermatids. M4 (N terminus of Brdt) was first checked for its chromatin reorganization property, because this domain is sufficient to bind to Smarce1. As observed in Fig. 10*A* (*panel I*), M4 could reorganize acetylated chromatin in treated nuclei much like the full-length Brdt protein (Fig. 4*A*) as compared with untreated nuclei (Fig. 10*B, panel I*). When the status of endogenous Smarce1 was probed using anti-Smarce1 antibody, an interesting phenomenon was observed. The colocalization of Smarce1 with M4 increased dramatically in the treated nuclei (Fig. 10, *A* and *B*, *panel II*). To ensure that the signal for M4 was not coming from endogenous Brdt, M4 was probed with anti-FLAG antibody and not the anti-Brdt antibody. To quantify this colocalization, a scatter plot analysis was done. As seen in *panel III* of Fig. 10, *A* and *B*, the colocalized pixels shown in the third quadrant of the scatter plot are much higher in HDAC inhibitor-treated nuclei. This is complemented by the cut mask image of treated and untreated nuclei in *panel IV* (Fig. 10, *A* and *B*) showing only the colocalized pixels. When the data from three independent experiments was plotted, the percentage of colocalized pixels (of M4 and Smarce1) showed an increase by ~15-fold in the treated nuclei (over untreated nuclei) (Fig. 10*C*).

To carry this result forward, we performed remodeling assays in total testicular nuclei from a 45-day-old-rat followed by pulldown of M4 by M2-agarose beads. Multiple reactions after pulldown from treated and untreated nuclei were pooled and immunoblotted using antibodies against Smarce1, acetylated H4, and β-actin. All these proteins showed enrichment in samples from treated nuclei as compared with untreated nuclei (Fig. 10*D*). The blot was reprobed with anti-FLAG antibody to ensure equal loading of M4. The blots were incubated with antibodies against α-tubulin and GAPDH as controls, which did not show any interaction with M4. The blots were developed using West Femto kit (Thermo Scientific), which can detect proteins in femtograms. None of the blots except for M4 showed any signal with the West Pico kit (Thermo Scientific), which is less sensitive.

DISCUSSION

A salient feature of mammalian spermiogenesis is the global chromatin remodeling that takes place in spermatids whereby

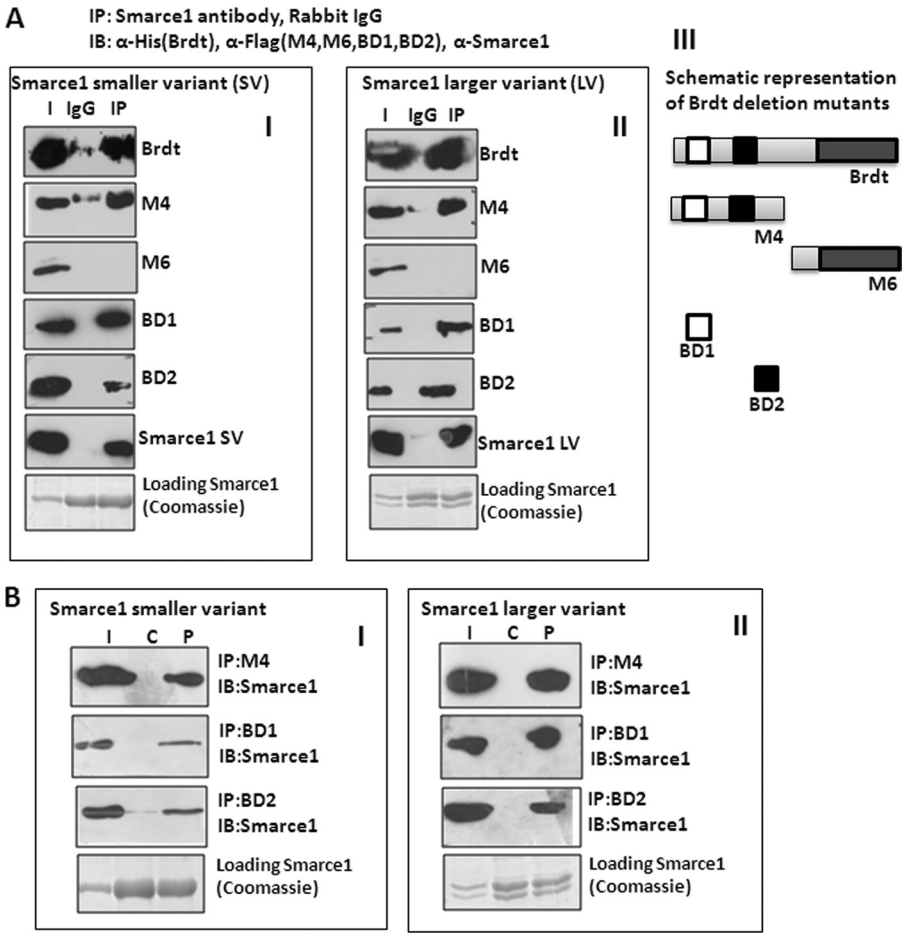

FIGURE 8. **Brdt interacts with Smarce1 through its N terminus *in vitro*.** *A, in vitro* immunoprecipitation (*IP*) experiments were performed using Smarce1 antibody and mock rabbit IgG (*IgG*) as control. *I* is the input lane representing 20% of the protein sample added to the reaction. Experiments were performed in parallel for Smarce1 smaller variant (*panel I*) and larger variant (*panel II*). Brdt was detected by α-His antibody. Immunoblotting (*IB*) with α-FLAG antibody was used to detect partial constructs of Brdt- M4 (N terminus), M6 (C terminus), BD1 (first bromodomain), and BD2 (second bromodomain). Smarce1 pulldown was probed with α-Smarce1 antibody, and a Coomassie Blue-stained gel of Smarce1 indicates equal loading. *Panel III* shows the schematic domain architecture of Brdt and its deletion mutants. *B,* reverse FLAG-tag pulldown. *Panels I* and *II* show reactions performed for Smarce1 smaller variant and larger variant, respectively. Brdt mutants M4, BD1, and BD2 were immunoprecipitated using FLAG M2-agarose beads, and immunoblotting was done using α-Smarce1 antibody. In each case, the deletion mutants were probed with α-FLAG antibody to confirm the pulldown (data not shown). Coomassie Blue-stained gel of Smarce1 depicts equal loading. *I*, 20% input protein; *C,* pulldown of Smarce1 with only beads as control; *P,* pulldown of Smarce1 with Brdt mutants.

histones from 85 to 90% of the chromatin are replaced by protamines. This study was initiated to identify the chromatin remodeling factors that take part in this process. Of the 30 remodeling factors analyzed, 22 were expressed in tetraploid spermatocytes. This is not surprising as pachytene spermatocytes are very active in recombination, transcription, and other chromatin-templated nuclear events, where chromatin remodeling factors presumably play a major role. However, we chose to focus on the 13 remodeling factors expressed in haploid spermatids with the assumption that the factors that are overexpressed in haploid round spermatids may play an important role in chromatin remodeling in the elongating stages of spermiogenesis as well. To our knowledge, this is the first comparative study of expression of chromatin remodeling factors in different spermatogenic cells. We narrowed it down to Brd2, Brdt, Baz2a, Smarca2, and Smarce1 based on real time RT-PCR analysis. While Brdt was present in the elongating stages of spermiogenesis, Brd2 protein expression was restricted to round spermatids only. Brdt expression reported in this study is slightly different from the one reported by Shang *et al.* (61). Although upon deletion of the first bromodomain they did see anomalies in sperm morphology, they were unable to detect Brdt in the elongating spermatids from normal mice, which could be due to the low sensitivity of the immunohistochemistry experiments. Brdt is not a highly immunogenic protein making it difficult to raise antibodies against it. With the peptide antibody raised in our laboratory, the detection of Brdt was possible even in the elongating spermatids when used at the appropriate concentration. Additionally, the cells were swollen in DTT before performing immunocytochemistry, which enhances the accessibility of the antibody to nuclear proteins in the condensing spermatids (24). This result is further corroborated by a recent report demonstrating the presence of Brdt in humans from spermatocytes to mature spermatozoa (62). In accordance with the results of Pivot-Pajot *et al.* (22), the acetylation-dependent chromatin reorganization property of Brdt could be re-demonstrated in RAG cells. However, in our case full-length Brdt was used, instead of the truncated version of murine Brdt (sBrdt) used by them. Interestingly, the additional C terminus did not have any effect on this activity. Additionally,

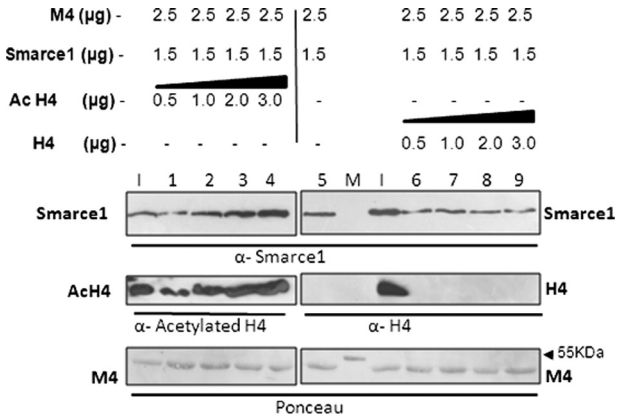

FIGURE 9. **A dose-dependent increase in interaction of Smarce1 with Brdt in the presence of acetylated H4.** An *in vitro* experiment was performed to check the effect of acetylated H4 on interaction between Smarce1 and Brdt. The concentrations of M4 (Brdt N terminus) and Smarce1 were kept constant, whereas the concentration of acetylated H4 was increased from 0.5 to 3 μg (*lanes 1–4*). An increase in the Smarce1 pulldown by M4 is observed upon increasing acetylated H4 concentration. No such enhanced interaction is observed upon increasing unacetylated H4 concentration (*lanes 6–9*). *Lane 5* represents interaction between Smarce1 and M4 (without H4). A dose-dependent increase in the pulldown of acetylated H4 is seen in *lanes 1–4,* but no corresponding bands are seen for unacetylated H4 (*lanes 6–9*). A Ponceau stained image of M4 depicts equal loading. *M,* marker; *I,* input (50%).

despite the presence of a Walker A-like motif in its C terminus, Brdt did not possess ATPase activity. The apparent role of the Brdt C terminus thus has yet not been elucidated and will be the subject matter of future investigation.

A wave of histone acetylation occurs in mammalian spermiogenesis in several organisms such as *Drosophila* (63, 64), trout (65, 66), rooster (67), rat (20, 21), mouse (68), and humans (69). In *Drosophila* (64) and mouse (70), histones fail to be replaced from the chromatin in the absence of histone H4 acetylation. Several DNA breaks also appear following histone acetylation and replacement, which are indicative of histone replacement (63). In species such as winter flounder (71) and grass carp (72) where histones are retained in spermiogenesis, they remain under-acetylated. These examples suggest a definite link between histone acetylation and their removal. Histone hyperacetylation is exclusive of transcription in haploid germ cells, unlike in somatic cells, and may have a context-dependent role in spermiogenesis that is manifested by germ cell-specific effector proteins. Brdt is a testis-specific double bromodomain containing chromatin remodeling factors shown to overexpress in haploid spermatids. Brdt can recognize both diacetylated (H4AcK5 and -8) and tetraacetylated (H4AcK5, -8, -12, and -16) H4 N terminus with equal affinity (31). This led us to the question if Brdt and acetylated H4 have intertwined roles in spermiogenesis. To test this, we first checked for any colocalization between them. Although colocalization was negligible in round spermatids, it increased dramatically in the early elongating spermatids (13.1%) and furthermore in the mid-elongating spermatids (19.8%). Colocalization was observed in elongating spermatids predominantly in the anterior region where the wave of histone acetylation/displacement begins (21). We next wanted to know the significance of this colocalization *in vivo*. Remodeling assays in round spermatids showed again an acetylation-dependent but ATP-independent activity of Brdt. Taking cues from earlier work by Pivot-Pajot *et al.* (22), it was shown that the N terminus of Brdt (M4) was enough to perform this activity. However, as reported by their group, we did not find any increase in the activity upon C-terminal deletion. This could be due to factors present exclusively in germ cells that regulate this activity, placing our study on chromatin changes in the naturally relevant system (haploid spermatids) into perspective. To know which other accessory factors associate with Brdt for its functional manifestation, immunoprecipitation with anti-Brdt antibody was done from total testicular nuclear extracts. We picked Smarce1 as an interesting interacting partner because of its overexpression in haploid spermatids and also because it is a member of the SWI/SNF family of remodelers that are known for histone eviction activity. Upon performing expression analysis in spermatogenic cells, we could identify two splice variants of Smarce1. Brdt could interact with both the variants through its N terminus. Interestingly, both the bromodomains (BD1 and BD2) of Brdt could recognize Smarce1 as well, hinting at the possibility of multiple points of interaction between Brdt and Smarce1. This is the first report showing bromodomains of Brdt can also bind to unacetylated substrates, although the structural details of this interaction have not been addressed in this study. Even though both Smarce1 variants can interact with Brdt *in vitro*, the smaller variant is more prominent in the sonication-resistant spermatids (elongating and condensing spermatid stages) and could be the Brdt interacting partner in these stages. Smarce1 was one of the five remodelers seen overexpressing in haploid spermatids, indicating a coordinated expression of chromatin remodeling factors that participate in later stages of spermiogenesis.

Another interesting observation that was made in this study is the status of endogenous Smarce1 in round spermatids when analyzed upon performing remodeling assay with M4. The colocalization of Smarce1 was seen to increase by almost 15-fold in the nuclei of cells treated with HDAC inhibitors. The extent of colocalization was ~25–30% (but never 100%) upon treatment as compared with 2–5% in the untreated nuclei. This result was validated *in vitro* by observation of an enhanced interaction between Smarce1 and M4 in the presence of acetylated H4. Smarce1 belongs to the SWI/SNF family of Brg-1-associated factors and is known to be a part of multimeric ATP-dependent chromatin remodeling complexes regulating subunit interactions (52, 55). It has a DNA binding high mobility group domain and is known to specify targeting of the SWI/SNF complexes (51, 73). In this context, it is worth mentioning here that there are several examples available in literature where post-translational modifications on histones lead to the recruitment of a chromatin remodeling complex (74).

Based on these results, we propose a model for chromatin remodeling in spermiogenesis (Fig. 11). The round spermatid chromatin is represented in Fig. 11 at the dinucleosome level, where salt bridges and H-bonds between H4 and H2A-H2B dimer on neighboring nucleosomes provide a compact chromatin structure as is known from the crystal structure of the nucleosome (2). In the early elongating spermatids drastic hyperacetylation of histone H4 occurs, where H4 becomes acetylated on lysine at positions 5, 8, 12, and 16. Of the four lysine residues that are acetylated, H4K16 acetylation is generally associated with decompaction of chromatin, as this acety-

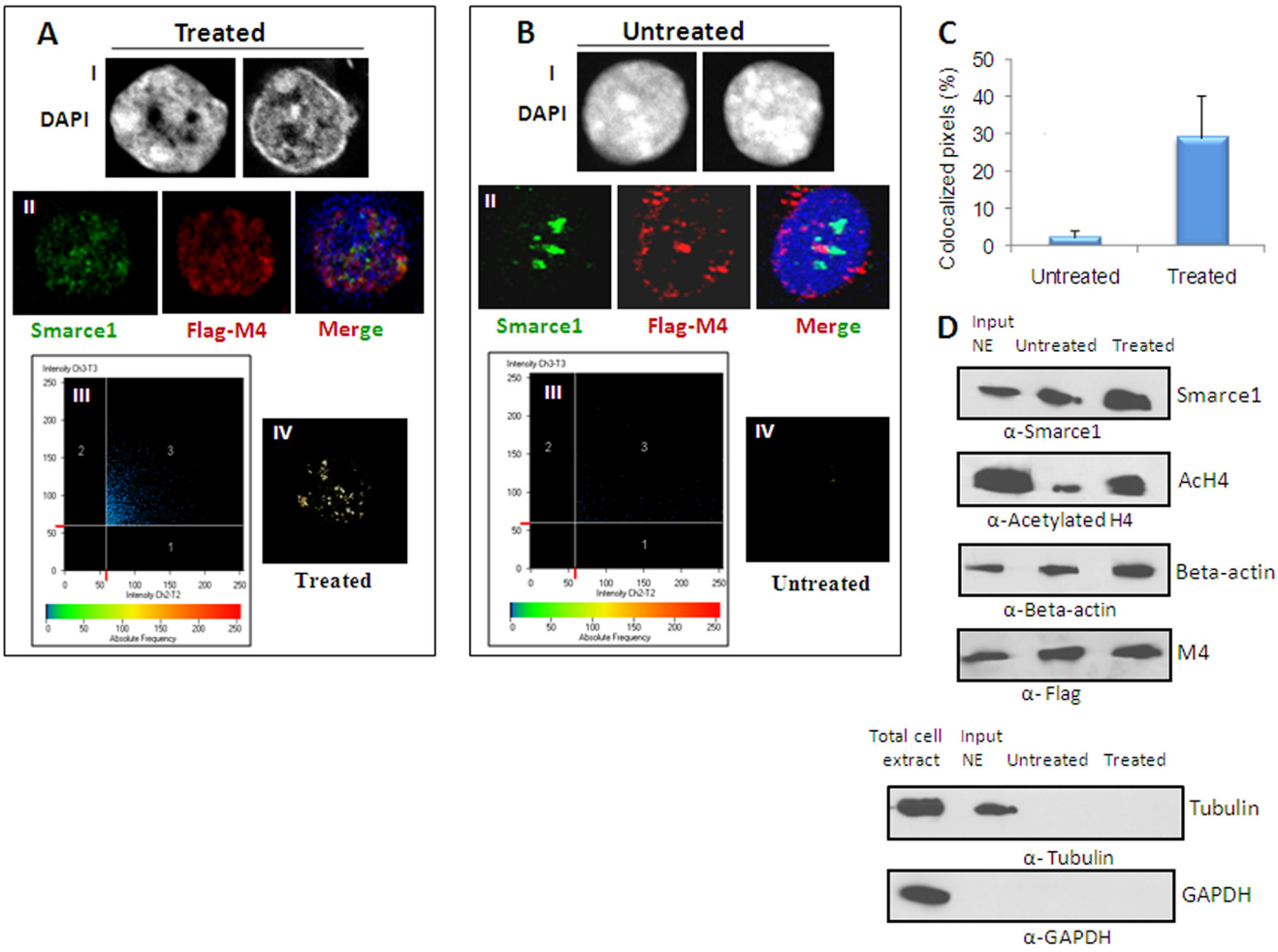

FIGURE 10. **N terminus of Brdt (M4) recruits endogenous Smarce1 to acetylated chromatin in round spermatids.** *A* and *B* show treated and untreated round spermatid nuclei, respectively. In each case, *panel I* shows changes in chromatin reorganization (visualized by DAPI) brought about by M4. Although the nuclei of untreated cells remained unaltered upon M4 addition, chromatin of treated nuclei showed reorganization. *Panel II* depicts the colocalization of endogenous Smarce1 with FLAG-M4. *Columns* from *left to right* show fluorescent signals obtained from Smarce1, FLAG-M4, and Merge (DAPI/Smarce1/FLAG-M4). It was observed that the colocalization of Smarce1 with M4 increased upon hyperacetylation of the chromatin. The scatter plot is shown in *panel III*, in which Smarce1 and FLAG-M4 colocalized pixels are represented in quadrant 3. *Panel IV* represents the cut mask image of nuclei (from *panel II*) showing only colocalized pixels. *C,* data of Smarce1 and FLAG-M4 colocalization from three independent experiments are plotted in a graph, showing the percentage of colocalized pixels increases upon treatment of round spermatids with HDAC inhibitors (NaBu and TSA). *D,* pulldown experiments were performed on nuclei following remodeling assay. An increased pulldown of Smarce1, acetylated H4 (*AcH4*), and β-actin was observed in the nuclei of treated round spermatids compared with untreated nuclei. *M4* represents equal pulldown in treated and untreated nuclei. *Input NE* represents 20% of the nuclear extracts. Tubulin and GAPDH were used as negative controls for the pulldown reactions.

lation disrupts the H-bonds and salt bridges between the adjoining nucleosomes in nucleosome arrays (75). H4K16 acetylation is also a very critical histone post-translational modification in spermiogenesis, as a recent report has shown that the absence of this modification leads to retention of histones in the chromatin of mature sperms (70). Although the acetylation of H4K16 remains constitutive, lysine 5, 8, and 12 acetylation progressively increases during differentiation in spermiogenesis. This increase in acetylation status of chromatin in elongating spermatids may be the combinatorial signal required for recruitment of Brdt, because although acetylation can loosen the chromatin slightly, it is not enough for histone removal and replacement (3). The H4 acetylation mark thus recruits a reader protein Brdt, which then reorganizes the chromatin to prepare it for further remodeling. Our data clearly shows that Brdt recognizes acetylated H4 starting from early elongating spermatids, increasing further in the mid-elongating spermatids. However, interaction between Smarce1 and Brdt happens one phase later, only in the mid-elongating stages. This indicates that upon hyperacetylation of H4, Brdt first binds acetylated H4 and then recruits Smarce1. Smarce1 is known to be a subunit of the SWI/SNF family of ATP-dependent chromatin remodelers. Immuno-pulldown performed on treated nuclei following remodeling assay with Brdt also showed an enhanced interaction with β-actin, another protein that was picked in our immunoprecipitation experiments with total testicular nuclear extracts. β-Actin is known to be a part of the human BAF and PBAF ATP-dependent chromatin remodeling complexes, much like Smarce1 (74). Smarce1 could be a part of such a complex that is recruited by Brdt to acetylated H4. Additionally, because the reorganization property of Brdt is ATP-independent, we propose Smarce1 and other member of the complex could be recruited by Brdt after it binds to acetylated H4 and reorganizes the chromatin for further remodeling.

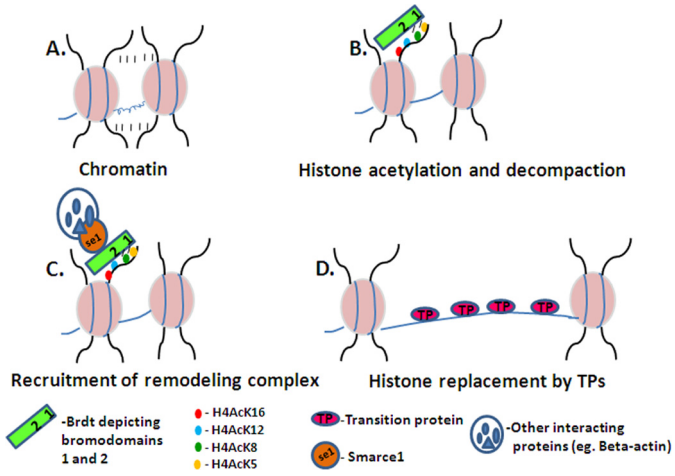

FIGURE 11. **Model proposing the mechanism of chromatin remodeling in spermiogenesis.** *A,* chromatin is represented at the dinucleosome level, where histone H4 in one nucleosome interacts with H2A-H2B dimer of the neighboring nucleosome by H-bonds and salt bridges. *B,* wave of H4-hyperacetylation begins in the early elongating spermatids, acetylating H4 at lysines 5, 8, 12, and 16. This mark is recognized by a double bromodomain containing protein, Brdt, via its first bromodomain. *C,* Brdt reorganizes the acetylated chromatin and further recruits Smarce1 and other interacting proteins (*e.g.* β-actin). *D,* finally the histones are removed from the chromatin and replaced by transition proteins (*TP*) (10% of histones are retained).

Other members of the BET family Brd2 and Brd4 have also been shown to be a part of chromatin remodeling complexes involved in transcriptional regulation in somatic cells (30). In one such Brd2 transcription complex, Smarca4 (Brg-1) is a component of the multisubunit complex (76). Interestingly, of the two subunits (Smarca2/Brm and Smarca4/Brg-1) of the SWI/SNF family that gave the remodeling complex its characteristic ATPase activity, Smarca2 is overexpressed in haploid spermatids, much like Brdt and Smarce1 (real time RT-PCR). Smarca4, although not overexpressed, is nonetheless highly expressed in round spermatids. Although we did not pick any other members of the SWI/SNF remodelers in our pulldown experiments through mass spectrometry, we did find a few proteins that are involved in nucleosome disassembly, DNA end joining and repair, which are other major events taking place during histone removal in spermiogenesis. Hence, it becomes imperative to identify and characterize the Brdt chromatin remodeling complex from haploid spermatids to further our understanding of the molecular mechanisms involved in the global remodeling phenomenon associated with histone eviction that is very unique to mammalian spermiogenesis, and this is presently being investigated in our laboratory.

Acknowledgments—We thank B. S. Suma and G. Roopa for help with confocal microscopy and MS/MS analysis, respectively. We thank Divya Sinha from the Shogren-Knaak laboratory for providing the p208-12 plasmid and Prof. Kondaiah for providing the β-actin antibody. We also thank to Tushna Dehnugara for help with culturing of round spermatids.

REFERENCES

1. Kornberg, R. D. (1974) Chromatin structure. A repeating unit of histones and DNA. *Science* **184,** 868–871
2. Luger, K., Mäder, A. W., Richmond, R. K., Sargent, D. F., and Richmond, T. J. (1997) Crystal structure of the nucleosome core particle at 2.8 Å resolution. *Nature* **389,** 251–260
3. Peterson, C. L., and Laniel, M. A. (2004) Histones and histone modifications. *Curr. Biol.* **14,** R546–R551
4. Shahbazian, M. D., and Grunstein, M. (2007) Functions of site-specific histone acetylation and deacetylation. *Annu. Rev. Biochem.* **76,** 75–100
5. Jenuwein, T., and Allis, C. D. (2001) Translating the histone code. *Science* **293,** 1074–1080
6. Turner, B. M. (2002) Cellular memory and the histone code. *Cell* **111,** 285–291
7. Kouzarides, T. (2007) Chromatin modifications and their function. *Cell* **128,** 693–705
8. Bannister, A. J., and Kouzarides, T. (2011) Regulation of chromatin by histone modifications. *Cell Res.* **21,** 381–395
9. Winston, F., and Allis, C. D. (1999) The bromodomain. A chromatin-targeting module? *Nat. Struct. Biol.* **6,** 601–604
10. Yap, K. L., and Zhou, M. M. (2011) Structure and mechanisms of lysine methylation recognition by the chromodomain in gene transcription. *Biochemistry* **50,** 1966–1980
11. Fischle, W. (2008) Talk is cheap. Cross-talk in establishment, maintenance, and readout of chromatin modifications. *Genes Dev.* **22,** 3375–3382
12. Wouters-Tyrou, D., Martinage, A., Chevaillier, P., and Sautière, P. (1998) Nuclear basic proteins in spermiogenesis. *Biochimie* **80,** 117–128
13. Sassone-Corsi, P. (2002) Unique chromatin remodeling and transcriptional regulation in spermatogenesis. *Science* **296,** 2176–2178
14. Lewis, J. D., Abbott, D. W., and Ausió, J. (2003) A haploid affair. Core histone transitions during spermatogenesis. *Biochem. Cell Biol.* **81,** 131–140
15. Govin, J., Caron, C., Lestrat, C., Rousseaux, S., and Khochbin, S. (2004) The role of histones in chromatin remodeling during mammalian spermiogenesis. *Eur. J. Biochem.* **271,** 3459–3469
16. Boussouar, F., Rousseaux, S., and Khochbin, S. (2008) A new insight into male genome reprogramming by histone variants and histone code. *Cell Cycle* **7,** 3499–3502
17. Carrell, D. T., and Hammoud, S. S. (2010) The human sperm epigenome and its potential role in embryonic development. *Mol. Hum. Reprod.* **16,** 37–47
18. Tan, M., Luo, H., Lee, S., Jin, F., Yang, J. S., Montellier, E., Buchou, T., Cheng, Z., Rousseaux, S., Rajagopal, N., Lu, Z., Ye, Z., Zhu, Q., Wysocka, J., Ye, Y., Khochbin, S., Ren, B., and Zhao, Y. (2011) Identification of 67 histone marks and histone lysine crotonylation as a new type of histone modification. *Cell* **146,** 1016–1028
19. Montellier, E., Rousseaux, S., Zhao, Y., and Khochbin, S. (December 15, 2011) Histone crotonylation specifically marks the haploid male germ cell gene expression program: post-meiotic male-specific gene expression. *BioEssays* 10.1002/bies.201100141
20. Grimes, S. R., Jr., and Henderson, N. (1984) Hyperacetylation of histone H4 in rat testis spermatids. *Exp. Cell Res.* **152,** 91–97
21. Meistrich, M. L., Trostle-Weige, P. K., Lin, R., Bhatnagar, Y. M., and Allis, C. D. (1992) Highly acetylated H4 is associated with histone displacement in rat spermatids. *Mol. Reprod. Dev.* **31,** 170–181
22. Pivot-Pajot, C., Caron, C., Govin, J., Vion, A., Rousseaux, S., and Khochbin, S. (2003) Acetylation-dependent chromatin reorganization by BRDT, a testis-specific bromodomain-containing protein. *Mol. Cell. Biol.* **23,** 5354–5365
23. Sudhakar, L., and Rao, M. R. (1990) Stage-dependent changes in localization of a germ cell-specific lamin during mammalian spermatogenesis. *J. Biol. Chem.* **265,** 22526–22532
24. Kolthur-Seetharam, U., Pradeepa, M. M., Gupta, N., Narayanaswamy, R., and Rao, M. R. (2009) Spatiotemporal organization of AT- and GC-rich DNA and their association with transition proteins TP1 and TP2 in rat condensing spermatids. *J. Histochem. Cytochem.* **57,** 951–962
25. Dehnugara, T., Dhar, S., and Rao, M. R. (2012) An *in vitro*, short term culture method for mammalian haploid round spermatids amenable for molecular manipulation. *Mol. Reprod. Dev.* **79,** 19–30
26. Meetei, A. R., Ullas, K. S., Vasupradha, V., and Rao, M. R. (2002) Involvement of protein kinase A in the phosphorylation of spermatidal protein

TP2 and its effect on DNA condensation. *Biochemistry* **41,** 185–195
27. Pradeepa, M. M., Nikhil, G., Hari Kishore, A., Bharath, G. N., Kundu, T. K., and Rao, M. R. (2009) Acetylation of transition protein 2 (TP2) by KAT3B (p300) alters its DNA condensation property and interaction with putative histone chaperone NPM3. *J. Biol. Chem.* **284,** 29956–29967
28. Shipra, A., Chetan, K., and Rao, M. R. (2006) CREMOFAC. A database of chromatin remodeling factors. *Bioinformatics* **22,** 2940–2944
29. Pradeepa, M. M., Manjunatha, S., Sathish, V., Agrawal, S., and Rao, M. R. (2008) Involvement of importin-4 in the transport of transition protein 2 into the spermatid nucleus. *Mol. Cell. Biol.* **28,** 4331–4341
30. Wu, S. Y., and Chiang, C. M. (2007) The double bromodomain-containing chromatin adaptor Brd4 and transcriptional regulation. *J. Biol. Chem.* **282,** 13141–13145
31. Morinière, J., Rousseaux, S., Steuerwald, U., Soler-López, M., Curtet, S., Vitte, A. L., Govin, J., Gaucher, J., Sadoul, K., Hart, D. J., Krijgsveld, J., Khochbin, S., Müller, C. W., and Petosa, C. (2009) Cooperative binding of two acetylation marks on a histone tail by a single bromodomain. *Nature* **461,** 664–668
32. Durrin, L. K., Mann, R. K., Kayne, P. S., and Grunstein, M. (1991) Yeast histone H4 N-terminal sequence is required for promoter activation *in vivo*. *Cell* **65,** 1023–1031
33. Kuo, M. H., Zhou, J., Jambeck, P., Churchill, M. E., and Allis, C. D. (1998) Histone acetyltransferase activity of yeast Gcn5p is required for the activation of target genes *in vivo*. *Genes Dev.* **12,** 627–639
34. Reid, J. L., Iyer, V. R., Brown, P. O., and Struhl, K. (2000) Coordinate regulation of yeast ribosomal protein genes is associated with targeted recruitment of Esa1 histone acetylase. *Mol. Cell* **6,** 1297–1307
35. Gerton, G. L., and Millette, C. F. (1984) Generation of flagella by cultured mouse spermatids. *J. Cell Biol.* **98,** 619–628
36. Aslam, I., and Fishel, S. (1998) Short term *in vitro* culture and cryopreservation of spermatogenic cells used for human *in vitro* conception. *Hum. Reprod.* **13,** 634–638
37. Champoux, J. J. (2001) DNA topoisomerases. Structure, function, and mechanism. *Annu. Rev. Biochem.* **70,** 369–413
38. Durand-Dubief, M., Persson, J., Norman, U., Hartsuiker, E., and Ekwall, K. (2010) Topoisomerase I regulates open chromatin and controls gene expression *in vivo*. *EMBO J.* **29,** 2126–2134
39. Straub, T., Knudsen, B. R., and Boege, F. (2000) PSF/p54(nrb) stimulates "jumping" of DNA topoisomerase I between separate DNA helices. *Biochemistry* **39,** 7552–7558
40. Bladen, C. L., Udayakumar, D., Takeda, Y., and Dynan, W. S. (2005) Identification of the polypyrimidine tract binding protein-associated splicing factor·p54(nrb) complex as a candidate DNA double strand break rejoining factor. *J. Biol. Chem.* **280,** 5205–5210
41. Chichiarelli, S., Ferraro, A., Altieri, F., Eufemi, M., Coppari, S., Grillo, C., Arcangeli, V., and Turano, C. (2007) The stress protein ERp57/GRP58 binds specific DNA sequences in HeLa cells. *J. Cell. Physiol.* **210,** 343–351
42. Krynetskaia, N. F., Phadke, M. S., Jadhav, S. H., and Krynetskiy, E. Y. (2009) Chromatin-associated proteins HMGB1/2 and PDIA3 trigger cellular response to chemotherapy-induced DNA damage. *Mol. Cancer Ther.* **8,** 864–872
43. Chichiarelli, S., Gaucci, E., Ferraro, A., Grillo, C., Altieri, F., Cocchiola, R., Arcangeli, V., Turano, C., and Eufemi, M. (2010) Role of ERp57 in the signaling and transcriptional activity of STAT3 in a melanoma cell line. *Arch. Biochem. Biophys.* **494,** 178–183
44. Gruppi, C. M., and Wolgemuth, D. J. (1993) HSP86 and HSP84 exhibit cellular specificity of expression and coprecipitate with an HSP70 family member in the murine testis. *Dev. Genet.* **14,** 119–126
45. Grad, I., Cederroth, C. R., Walicki, J., Grey, C., Barluenga, S., Winssinger, N., De Massy, B., Nef, S., and Picard, D. (2010) The molecular chaperone Hsp90α is required for meiotic progression of spermatocytes beyond pachytene in the mouse. *PLoS One* **5,** e15770
46. Chi, M. N., Auriol, J., Jégou, B., Kontoyiannis, D. L., Turner, J. M., de Rooij, D. G., and Morello, D. (2011) The RNA-binding protein ELAVL1/HuR is essential for mouse spermatogenesis, acting both at meiotic and postmeiotic stages. *Mol. Biol. Cell* **22,** 2875–2885
47. Hui, J., Stangl, K., Lane, W. S., and Bindereif, A. (2003) HnRNP L stimulates splicing of the eNOS gene by binding to variable-length CA repeats. *Nat. Struct. Biol.* **10,** 33–37
48. Hui, J., Hung, L. H., Heiner, M., Schreiner, S., Neumüller, N., Reither, G., Haas, S. A., and Bindereif, A. (2005) Intronic CA-repeat and CA-rich elements. A new class of regulators of mammalian alternative splicing. *EMBO J.* **24,** 1988–1998
49. Yu, J., Hai, Y., Liu, G., Fang, T., Kung, S. K., and Xie, J. (2009) The heterogeneous nuclear ribonucleoprotein L is an essential component in the Ca^{2+}/calmodulin-dependent protein kinase IV-regulated alternative splicing through cytidine-adenosine repeats. *J. Biol. Chem.* **284,** 1505–1513
50. Gozani, O., Patton, J. G., and Reed, R. (1994) A novel set of spliceosome-associated proteins and the essential splicing factor PSF bind stably to pre-mRNA prior to catalytic step II of the splicing reaction. *EMBO J.* **13,** 3356–3367
51. Belandia, B., Orford, R. L., Hurst, H. C., and Parker, M. G. (2002) Targeting of SWI/SNF chromatin remodeling complexes to estrogen-responsive genes. *EMBO J.* **21,** 4094–4103
52. Chen, J., and Archer, T. K. (2005) Regulating SWI/SNF subunit levels via protein-protein interactions and proteasomal degradation. BAF155 and BAF170 limit expression of BAF57. *Mol. Cell. Biol.* **25,** 9016–9027
53. Link, K. A., Balasubramaniam, S., Sharma, A., Comstock, C. E., Godoy-Tundidor, S., Powers, N., Cao, K. H., Haelens, A., Claessens, F., Revelo, M. P., and Knudsen, K. E. (2008) Targeting the BAF57 SWI/SNF subunit in prostate cancer. A novel platform to control androgen receptor activity. *Cancer Res.* **68,** 4551–4558
54. Kazantseva, A., Sepp, M., Kazantseva, J., Sadam, H., Pruunsild, P., Timmusk, T., Neuman, T., and Palm, K. (2009) N-terminally truncated BAF57 isoforms contribute to the diversity of SWI/SNF complexes in neurons. *J. Neurochem.* **109,** 807–818
55. Hah, N., Kolkman, A., Ruhl, D. D., Pijnappel, W. W., Heck, A. J., Timmers, H. T., and Kraus, W. L. (2010) A role for BAF57 in cell cycle-dependent transcriptional regulation by the SWI/SNF chromatin remodeling complex. *Cancer Res.* **70,** 4402–4411
56. Keppler, B. R., and Archer, T. K. (2010) Ubiquitin-dependent and ubiquitin-independent control of subunit stoichiometry in the SWI/SNF complex. *J. Biol. Chem.* **285,** 35665–35674
57. Zhao, K., Wang, W., Rando, O. J., Xue, Y., Swiderek, K., Kuo, A., and Crabtree, G. R. (1998) Rapid and phosphoinositol-dependent binding of the SWI/SNF-like BAF complex to chromatin after T lymphocyte receptor signaling. *Cell* **95,** 625–636
58. Shumaker, D. K., Kuczmarski, E. R., and Goldman, R. D. (2003) The nucleoskeleton. Lamins and actin are major players in essential nuclear functions. *Curr. Opin. Cell Biol.* **15,** 358–366
59. Blessing, C. A., Ugrinova, G. T., and Goodson, H. V. (2004) Actin and ARPs. Action in the nucleus. *Trends Cell Biol.* **14,** 435–442
60. Visa, N., and Percipalle, P. (2010) Nuclear functions of actin. *Cold Spring Harb or Perspect Biol.* **2,** a000620
61. Shang, E., Nickerson, H. D., Wen, D., Wang, X., and Wolgemuth, D. J. (2007) The first bromodomain of Brdt, a testis-specific member of the BET subfamily of double-bromodomain-containing proteins, is essential for male germ cell differentiation. *Development* **134,** 3507–3515
62. Barda, S., Paz, G., Yogev, L., Yavetz, H., Lehavi, O., Hauser, R., Botchan, A., Breitbart, H., and Kleiman, S. E. (2012) Expression of *BET* genes in testis of men with different spermatogenic impairments. *Fertil. Steril.* **97,** 46–52
63. Rathke, C., Baarends, W. M., Jayaramaiah-Raja, S., Bartkuhn, M., Renkawitz, R., and Renkawitz-Pohl, R. (2007) Transition from a nucleosome-based to a protamine-based chromatin configuration during spermiogenesis in *Drosophila*. *J. Cell Sci.* **120,** 1689–1700
64. Awe, S., and Renkawitz-Pohl, R. (2010) Histone H4 acetylation is essential to proceed from a histone- to a protamine-based chromatin structure in spermatid nuclei of *Drosophila melanogaster*. *Syst. Biol. Reprod. Med.* **56,** 44–61
65. Christensen, M. E., and Dixon, G. H. (1982) Hyperacetylation of histone H4 correlates with the terminal, transcriptionally inactive stages of spermatogenesis in rainbow trout. *Dev. Biol.* **93,** 404–415
66. Christensen, M. E., Rattner, J. B., and Dixon, G. H. (1984) Hyperacetylation of histone H4 promotes chromatin decondensation prior to histone replacement by protamines during spermatogenesis in rainbow trout. *Nu-*

cleic Acids Res. **12,** 4575–4592
67. Oliva, R., and Mezquita, C. (1982) Histone H4 hyperacetylation and rapid turnover of its acetyl groups in transcriptionally inactive rooster testis spermatids. *Nucleic Acids Res.* **10,** 8049–8059
68. Hazzouri, M., Pivot-Pajot, C., Faure, A. K., Usson, Y., Pelletier, R., Sèle, B., Khochbin, S., and Rousseaux, S. (2000) Regulated hyperacetylation of core histones during mouse spermatogenesis. Involvement of histone deacetylases. *Eur. J. Cell Biol.* **79,** 950–960
69. Faure, A. K., Pivot-Pajot, C., Kerjean, A., Hazzouri, M., Pelletier, R., Péoc'h, M., Sèle, B., Khochbin, S., and Rousseaux, S. (2003) Misregulation of histone acetylation in Sertoli cell-only syndrome and testicular cancer. *Mol. Hum. Reprod.* **9,** 757–763
70. Lu, L. Y., Wu, J., Ye, L., Gavrilina, G. B., Saunders, T. L., and Yu, X. (2010) RNF8-dependent histone modifications regulate nucleosome removal during spermatogenesis. *Dev. Cell* **18,** 371–384
71. Kennedy, B. P., and Davies, P. L. (1980) Acid-soluble nuclear proteins of the testis during spermatogenesis in the winter flounder. Loss of the high mobility group proteins. *J. Biol. Chem.* **255,** 2533–2539
72. Kadura, S. N., Khrapunov, S. N., Chabanny, V. N., and Berdyshev, G. D. (1983) Changes in chromatin basic proteins during male gametogenesis of grass carp. *Comp. Biochem. Physiol. B* **74,** 343–350
73. García-Pedrero, J. M., Kiskinis, E., Parker, M. G., and Belandia, B. (2006) The SWI/SNF chromatin remodeling subunit BAF57 is a critical regulator of estrogen receptor function in breast cancer cells. *J. Biol. Chem.* **281,** 22656–22664
74. Clapier, C. R., and Cairns, B. R. (2009) The biology of chromatin remodeling complexes. *Annu. Rev. Biochem.* **78,** 273–304
75. Shogren-Knaak, M., Ishii, H., Sun, J. M., Pazin, M. J., Davie, J. R., and Peterson, C. L. (2006) Histone H4-K16 acetylation controls chromatin structure and protein interactions. *Science* **311,** 844–847
76. Denis, G. V., McComb, M. E., Faller, D. V., Sinha, A., Romesser, P. B., and Costello, C. E. (2006) Identification of transcription complexes that contain the double bromodomain protein Brd2 and chromatin remodeling machines. *J. Proteome Res.* **5,** 502–511